# EXPRESSION AND REGULATION OF LET-7D IN IDIOPATHIC PULMONARY FIBROSIS

by

**Kusum Vijay Pandit**

M.B; B.S., University of Mumbai, 2001

Submitted to the Graduate Faculty of

Graduate School of Public Health in partial fulfillment

of the requirements for the degree of

Doctor of Philosophy

University of Pittsburgh

2010

UNIVERSITY OF PITTSBURGH

GRADUATE SCHOOL OF PUBLIC HEALTH

This dissertation was presented

by

Kusum Vijay Pandit

It was defended on

February 18, 2010

and approved by

Susanne Gollin, Ph.D., Professor, Department of Human Genetics,
Graduate School of Public Health, University of Pittsburgh

Eleanor Feingold, Ph.D., Associate Professor, Department of Human Genetics,
Graduate School of Public Health, University of Pittsburgh

Panayiotis Benos, Ph.D., Assistant Professor, Department of Computational Biology,
School of Medicine, University of Pittsburgh

Prabir Ray, Ph.D., Associate Professor, Department of Immunology, School of Medicine,
University of Pittsburgh

Dissertation Advisor: Naftali Kaminski, M.D., Associate Professor of Medicine,
Pathology, Human Genetics and Computational Biology, Division of Pulmonary,
Allergy, and Critical Care Medicine, University of Pittsburgh Medical Center

**EXPRESSION AND REGULATION OF LET-7D IN IDIOPATHIC PULMONARY FIBROSIS**

Kusum Vijay Pandit, PhD

University of Pittsburgh, 2010

Idiopathic pulmonary fibrosis (IPF) is a chronic, progressive, and usually lethal fibrotic lung disease with as yet unknown etiology and treatment. IPF lungs have a definitive gene expression signature, but the role of microRNAs in IPF has not been studied. MicroRNA genes are short, non-coding RNAs that function as post-transcriptional gene regulators. We hypothesized that microRNAs are differentially expressed in IPF and play a role in the pathogenesis of the disease.

The microRNA expression profile of IPF lungs was characterized using microRNA microarrays. We identified 18 significantly decreased and 28 significantly increased microRNAs in samples obtained from patients with IPF compared to controls. Promoter analysis of the decreased microRNAs recognized a SMAD3 binding site in the promoter of let-7d. SMAD3 binding and responsiveness to TGF-β of the let-7d promoter were confirmed by SMAD3 ChIP, EMSA, luciferase assays and reduced expression of let-7d in response to TGF-β. *In situ* hybridization confirmed a significant reduction in let-7d expression in IPF lungs and localized it to alveolar epithelial cells in the control lungs. To study the role of let-7d, we determined the consequences of loss of function of let-7d by inhibiting its expression in lung epithelial cells. *In-vitro* inhibition of let-7d caused increases in epithelial mesenchymal transition (EMT) markers N-cadherin (CDH2), vimentin (VIM), alpha-smooth muscle actin (ACTA2) and high mobility group AT-hook 2 (HMGA2). HMGA2 is a proven let-7d target that was increased in IPF lungs and localized to alveolar epithelial cells. We reproduced our *in vitro* results *in vivo*. In mice,

intratracheal administration of a let-7d inhibitor caused alveolar septal thickening, increases in collagen, ACTA2 and CDH2 and decreases in the epithelial markers, CDH1 and ZO1. We colocalized the mesenchymal markers FSP1 and ACTA2 with the epithelial marker SPC, indicative of EMT.

Our results indicate a definitive role for microRNAs in IPF. The downregulation of let-7d in IPF and the pro-fibrotic effects of this downregulation *in vitro* and *in vivo* suggest a key regulatory role for this microRNA in preventing lung fibrosis. Deciphering their mechanism of action of microRNAs has great public health significance. It would add new insight into the pathophysiology of the disease and aid in reducing the mortality by development of therapeutic interventions.

## TABLE OF CONTENTS

## LIST OF TABLES

## LIST OF FIGURES

# PREFACE

I would like to thank my mentor Dr. Naftali Kaminski for his constant guidance and support throughout my PhD. I cannot thank him enough for all the encouragement and advice. I am very grateful to my thesis committee members Dr. Susanne Gollin, Dr. Panayiotis Benos, Dr. Eleanor Feingold and Dr. Prabir Ray for their guidance and time.

Dozens of people have helped and taught me immensely at the Kaminski Laboratory over the past few years. I am indebted to them for providing me not only with scientific discussion, but also for providing support and encouragement during the course of this project. I would specially like to thank Mandal Singh, Guoying Yu, David Corcoran, Kazuhisa Konishi, Dan Handley, Manohar Yarlagadda, Melissa Paglia, Jadranka Milosevic, Lara Chensny, Mary Williams, Dale Lewis, Louis Vuga, Maria Kapetanaki, Giuseppe DeIuliis, Einat Rabinovich, Inna Loutaev and Elizabeta Naumovski-Kovkarova.

Finally, I would like to thank my husband, Rahul and my parents for their constant encouragement. With all their love and support it was easier for me to achieve this goal.

# 1.0 INTRODUCTION

Idiopathic pulmonary fibrosis (IPF) is a disease of unknown etiology and no proven treatment. Though there is a distinct gene expression signature of this disease, the microRNA profile has not been studied. MicroRNA profiles are altered in different types of cancers and also in benign diseases. We hypothesized that there exists a unique microRNA profile for IPF. Differentially expressed microRNAs will possibly be targeting some disease-relevant genes. The aim of this study was to identify these microRNAs and determine their role in the pathogenesis of IPF.

## 1.1 PUBLIC HEALTH SIGNIFICANCE

Idiopathic pulmonary fibrosis is a chronic, progressive and usually lethal interstitial lung disease [1]. The incidence of IPF in US is 16.3 per 100,000 persons with a median survival of 2.5-3 years from diagnosis [2]. The etiology and molecular mechanisms underlying the lung phenotype in IPF are largely unknown. A number of risk factors like smoking, infectious agents, drugs and genetic predisposition are thought to contribute to disease development [3, 4]. Currently, there is no known cure for this devastating disease. Clinical management focuses mainly on supportive care and in a few cases lung transplant. Though the gene expression of IPF has been studied [5-13], the contribution of changed expression of microRNAs to IPF is not known. MicroRNAs add

a new level of gene regulation to the already existing complex cellular networks. Deciphering their mechanism of action would add new insight into the pathophysiology of the disease and aid in therapeutic interventions.

## 1.2 IDIOPATHIC PULMONARY FIBROSIS

The 2002 international consensus classification of the idiopathic interstitial pneumonias (IIPs) recommended by the American Thoracic Society and European Respiratory Society [4] recognizes seven distinct clinicopathologic entities of which IPF is the most frequent. An international consensus statement regarding the diagnosis of IPF has been outlined [3]. The major criteria include (a) exclusion of other known causes of interstitial lung diseases, (b) abnormal pulmonary function tests indicative of restriction and abnormal gas exchange, (c) Bibasilar reticular abnormalities with minimal ground glass opacities on HRCT scans and (d) bronchoalveolar lavage does not support any other diagnosis. The minor criteria include (a) over 50 years, (b) gradual onset of shortness of breath, (c) symptoms persisting for more than 3 months and (d) bibasilar crackles on auscultation. All major criteria and at least 3 minor criteria are necessary for an accurate diagnosis of IPF. Histological characteristics of IPF lungs include increase in extracellular matrix deposition, honeycombing of the lung and the presence of myofibroblast foci.

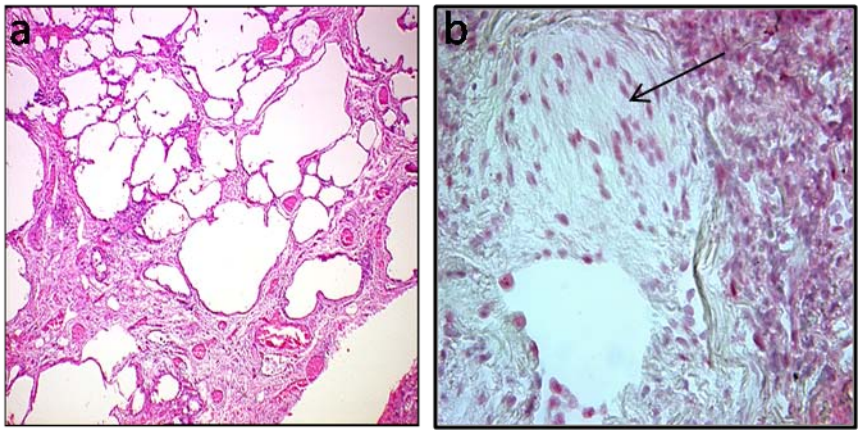


**Figure 1. Histolgical characteristics of IPF, (a) Honeycomb lung, (b) Fibroblast focus.**

Studying the disease in an animal model plays an important role in determining the pathobiology. Modeling IPF in an animal model is difficult since the etiology and the natural history of the disease is as yet uncertain and no single agent has been able to mimic IPF in animals. Common methods include radiation damage, instillation of bleomycin, silica or asbestos or gene transfer of fibrogenic cytokines. The most common method of inducing experimental pulmonary fibrosis is bleomycin instillation. Bleomycin is an anti-neoplastic drug with lung fibrosis being one of its side effects. The bleomycin-inactivating enzyme, bleomycin hydrolase, is present at low levels in lungs. Hence the lungs are more prone to bleomycin-induced fibrosis [14]. Following intratracheal instillation of bleomycin, there is an initial rise in inflammatory cytokines followed by an elevation in profibrotic markers which peaks around day 14 [15]. Histological hallmarks of IPF are seen in lungs of bleomycin-treated mice [16]. Bleomycin-induced fibrosis is partially reversible over time [17]. The slow and irreversible progression of IPF is not reproduced in the bleomycin model.

### 1.2.1 Genetic Associations of IPF

The vast majority of IPF cases occur sporadically, a few cases being familial. Approximately one of every 50 patients with IPF has an affected first-degree family member [18, 19]. The clinical presentation of familial and sporadic IPF is similar, though familial IPF manifests earlier. Pulmonary fibrosis is also associated with a number of well-defined genetic disorders, including Hermansky-Pudlak Syndrome, Gaucher Disease and Familial Hypocalciuric Hypercalcemia [20-23]. This indicates some mode of inheritance of genes responsible for the development of pulmonary fibrosis.

Specific gene mutations are also observed in some patients. One such gene, surfactant protein C (*SFTPC*), codes for a hydrophobic membrane protein produced by alveolar type II epithelial cells. It works with other surfactant proteins (A, B, D) to reduce surface tension in the aqueous alveolar space and allows gas exchange. The mutations results in protein misfolding and consequent epithelial cell injury [24, 25]. A genetic mutation in surfactant protein A2 has now been identified in some familial cases of IPF.

Telomere reverse transcriptase (*hTERT*) is another gene which has an association with IPF. Telomeres contain multiple repeats of the TTAGGG sequence at the ends of chromosomes. Some of these repeat sequences are lost with each cell division. The telomerase enzyme encoded by *hTERT*, mediates addition of TTAGGG to replace those lost during cell division. Without the proper telomerase activity, telomeres will shorten to the point that cells will fail to divide [26]. Tsakiri *et al.,* conducted genome-wide linkage studies and identified a mutation in *hTERT* that co-segregated with idiopathic interstitial pneumonias in two families [27]. Those individuals with heterozygous mutations in *hTERT* or *hTERC* had shorter telomere lengths compared to controls [27, 28]. Short dysfunctional telomeres lead to cell death which manifests as organ

failure in tissues of high turnover. The bronchoalveolar epithelium is constantly being replaced and relies on local progenitor cells to be replaced which are limited by short telomeres. Armanios *et al*. propose that the fibrotic lesions and remodeling are a result of loss of alveolar epithelial cells [28]. Fortunately, these genetic mutations are known to have low penetrance suggesting that factors other than genetics contribute to the disease pathogenesis even in familial cases.

### 1.2.2 Pathophysiology of IPF

The initial model for the pathology suggested that chronic inflammation was the underlying cause of IPF [29, 30]. But since immunosuppressive drugs do not change the prognosis and measures of tissue inflammation correlate poorly to the outcome of the disease, an alternate hypothesis of epithelial injury was proposed.

Alveoli are lined by alveolar type I and type II cells. The type II cells cover about 5% of the surface. They secrete surfactant into the alveoli and differentiate into type I cells when the latter are injured. The type I cells cover about 95% of the alveolar surface and facilitate gas exchange. In IPF however, this normal mechanism of type I cell replacement is lost [31, 32]. The alveolar cells either undergo apoptosis or epithelial mesenchymal transition (EMT). The nature of the epithelial injury is unknown though it has been speculated that viral infections [33] or oxidative stress [34, 35] may play a role. The injured alveolar epithelium serves as a major source of TGF-β1 and many other cytokines including endothelin-1 and tumor necrosis factor-α [36–38] independent of pro-inflammatory mediators [39]. These profibrotic cytokines influence the neighbouring fibroblasts which in turn secrete reactive oxygen species, Fas and angiotensin-II further inducing epithelial cell injury and apoptosis [40]. Thus each cell type influences the survival and proliferation of the other. The alveolar epithelium also has an

intrinsic capacity to respond to TGF-β1 stimulation through differential expression of TGF-β1 receptor subtypes [41]. The epithelial cells overlying the fibroblastic foci are hyperplastic and dysplastic having an abnormal morphology and altered gene expression [42, 43]. Persistent injury to epithelial cells leading to the loss of the basement membrane integrity to an extent where normal repair cannot take place is essential for all the subsequent fibrotic events [44]. Matrix metalloproteinases (MMPs) are also secreted by injured epithelial cells. MMPs are capable of degrading various components of connective tissue matrices are believed to play a significant role in remodelling after parenchymal damage. MMPs can participate in the fibrotic process at two stages- at the injury stage by degrading the basement membrane and extracellular matrix constituents; and secondly at the "attempted repair" stage where the MMPs may contribute to increased accumulation of extracellular matrix components such as collagens, fibronectin, elastin and proteoglycans [45].

Increased apoptosis of type II cells has been demonstrated in areas that appear histologically normal [46] and in epithelial cells that near the myofibroblasts [47]. Increase in proapoptotic protein expression and a decrease in antiapoptotic proteins has been reported [48]. Mice developed lung fibrosis after they were administered aerosolized anti-Fas antibody [49]. It has recently been shown that activated myofibroblasts produce extracellular reactive oxygen species that is sufficient to induce apoptosis in adjacent epithelial cells [40]. However, the adjacent fibroblasts and myofibroblasts show little evidence of apoptosis [47, 48, 50]. Human lung fibroblasts express increased amounts of inhibitors of apoptosis such as XIAP and FLIP [51].

Another cytokine implicated in the pathogenesis of IPF is endothelin-1 (ET-1). ET-1 is the principal effector of the many profibrotic roles of TGF-β such as the differentiation of

fibroblasts to myofibroblasts [52], the production of altered ECM components [53], the inhibition of ECM degradation [52, 53] and in EMT [54]. Alveolar macrophages spontaneously secrete ET-1 in IPF when compared with control subjects [55, 56]. Serum and bronchoalveolar lavage from IPF patients has increased amounts of ET-1 [57, 58]. Immunohistochemical analysis of lung biopsies from IPF patients demonstrated increased staining for ET-1 especially in areas of active tissue remodeling [55]. Bleomycin-induced pulmonary fibrosis in the rat results in increased ET-1 and its receptor expression [59-61]. Also, transgenic mice that overexpress human pre–proET-1 and ET-1 transcriptional elements spontaneously develop progressive pulmonary fibrosis [62].

### 1.2.3 Gene expression studies of IPF

High throughput gene expression profiling studies have been conducted to determine the characteristic gene expression signature of IPF lungs. Gene expression patterns are distinct in fibrotic and non-fibrotic lungs [5-13] irrespective of the microarray platform used [6, 11, 12, 63]. Genes that encode proteins involved in extracellular matrix formation, degradation, and signaling such as matrix metalloproteinases, collagens I and III, osteopontin are increased in fibrotic lungs. Genes that encode immunoglobulins, complement, and some chemokines are also up-regulated in fibrotic lungs. Among the down-regulated genes is caveolin-1 [64] and advanced glycosylation end products-specific receptor (AGER) [65].

Recently, the gene expression data [6, 8, 11] has been reanalyzed [66]. The analysis revealed that IPF lungs were significantly enriched with genes associated with lung development. The up-regulated development-relevant genes included several members of transcription factor families such as the Sry-related high mobility group box and forkhead box,

and genes related to the Wnt/β-catenin pathway and many EMT-related genes. These pathways that play an essential role during embryological development are inactivated in adults but may be transiently expressed during wound repair. Aberrant activation of these pathways in adults may be associated with the development of IPF.

### 1.2.4 Origin and role of the myofibroblast

The myofibroblast plays a central role in the pathogenesis of IPF. Many myofibroblasts aggregate to form the fibroblastic focus, a characteristic histological hallmark of IPF. Increased numbers of these foci is associated with disease progression and a worse prognosis [67]. Examination of tissue sections suggest that fibrotic foci are isolated lesions, but Cool *et al*. demonstrated that the foci are a form of a highly complex, interconnected and continuous fibrotic reticulum [68]. The myofibroblast has a spindle-shaped morphology, intracytoplasmic stress fibers, and a contractile phenotype. It expresses the mesenchymal marker, α-smooth muscle actin and produces collagen [69]. Although myofibroblasts are a part of normal repair mechanisms, their persistence beyond a period of normal repair is associated with extracellular matrix deposition and structural remodeling [70]. Epithelial cells overlying the fibroblastic foci are hyperplastic and dysplastic with abnormal morphology and gene expression patterns [42, 43]. These cells serve as a major source of TGF-β and many other cytokines including endothelin-1 and TNF-α during lung injury [36, 38]. The increase of myofibroblasts in injured lungs has several deleterious effects, contributing to the abnormal alveolar re-epithelialization, and excessive and disordered deposition of extracellular matrix in the lung parenchyma. It has been demonstrated that IPF fibroblasts produce angiotensin peptides able to induce epithelial cell death *in vitro*, which also probably occurs *in v ivo* [47, 71]. In addition, IPF myofibroblasts

synthesize gelatinases A and B, two matrix metalloproteinases that degrade basement membrane molecules, contributing to the failure of an orderly repair of alveolar type I epithelial cells and enhancing the migration of fibroblasts/myofibroblasts into the alveolar spaces [72]. A number of hypotheses have been proposed regarding the origin of the myofibroblast.

The first theory proposes that resident lung fibroblasts respond to many stimuli and differentiate into myofibroblasts [70]. TGF-β induces transdifferentiation of fibroblasts *in vitro* through SMAD3 [73].

Another potential source of myofibroblasts is circulating mesenchymal progenitors or fibrocytes [74]. These are spindle-shaped cells that are likely bone marrow derived. They migrate to sites of tissue injury and can differentiate into fibroblast-like cells [75]. Fibrocytes express the common leukocyte antigen CD45, the hematopoietic stem cell antigen CD34 and mesenchymal markers such as collagen, fibronectin, alpha-smooth muscle actin and prolyl-4-hydroxylase. Transplantation of green fluorescent protein-positive bone marrow into wild type mice and subsequent induction of fibrosis in these mice by irradiation showed that about 20-50% of the cells in the fibrotic areas were bone marrow-derived [76]. Direkze *et al* [77] demonstrated multiple organ engraftments by bone marrow-derived fibroblasts and myofibroblasts in mice following radiation injury. Patients with IPF have an increased number of circulating fibrocytes [78]. Andersson-Sjoland *et al* demonstrated the presence of fibrocytes in lungs of IPF patients [79]. A subsequent study showed that fibrocytes were significantly elevated in stable IPF with a further increase in acute exacerbations of the disease and can be used as a clinical marker for disease progression [80].

Recently it has been proposed that alveolar epithelial cells (AEC) undergo epithelial-mesenchymal transition (EMT) to form fibroblasts. It has also been proposed that ongoing AEC

injury and retarded wound repair may be central to the pathogenesis of IPF. The authors showed that epithelial injury and blunted epithelial repair is sufficient to promote the pulmonary fibrotic process [81]. The exact nature of the epithelial injury is unknown, but viral infection may play a role. Depending on the nature of injury and extent of disruption of the basement membrane, injured AECs may undergo apoptosis, proliferate and differentiate into type I AEC to effect re-epithelialization or may undergo EMT and hence contribute directly to fibrosis. Kim et al. demonstrated EMT in the lungs of mice [82]. Mice expressing β-galactosidase (β-gal) exclusively in lung epithelial cells were generated and the mice were administered adenoviral active TGF-β1. β-gal-positive cells expressing mesenchymal markers accumulated within 3 weeks of in vivo TGF-β1 expression. In a subsequent publication they showed that α3 integrin was required for β-catenin phosphorylation at tyrosine residue 654, formation of the pY654–β-catenin/pSmad2 complex, and initiation of EMT [83]. Tanjore *et al*. [84] showed using cell fate reporter mice that approximately one-third of S100A4-positive fibroblasts were derived from lung epithelium and one-fifth of S100A4-positive fibroblasts were derived from bone marrow 2 weeks after bleomycin administration.

### 1.2.5 Signaling pathways in IPF

Progressive pulmonary fibrosis is a disorder of dysregulated cytokine production which subsequently leads to activation of different signaling pathways. A number of different pathways are involved in the pathogenesis of IPF, the most important being the TGF-β signaling pathway and the Wnt-β-catenin pathway.

#### 1.2.5.1 TGF-β signaling pathway

TGF-β inhibits epithelial growth, acting as a tumor suppressor but it also promotes carcinoma progression and metastasis. TGF-β binds to the type II receptor which phosphorylates the type I receptor. This causes phosphorylation of SMAD2 and SMAD3 which alongwith the common mediator SMAD4 are translocated to the nucleus and results on transcriptional activation or inhibition of target genes [85].

Many studies prove that TGF-β is the main cytokine in the pathogenesis of IPF. Increased expression of TGF-β mRNA and protein has been detected in the interstitial matrix and myofibroblasts found in areas of active extracellular matrix deposition in fibrotic foci of IPF patients [37, 86-90]. Alveolar macrophages secrete TGF-β in both humans and bleomycin-induced mouse model of fibrosis [88, 90].

Adenoviral-vector mediated gene transfer of TGF-β into rats induced histological changes similar to those seen in IPF patient lungs. There is increased extracellular matrix formation, destruction of the normal lung architecture and the characteristic honeycombing [91, 92]. Nuclear SMAD3 increased in bleomycin-treated mice lungs [93] whereas SMAD3 knockout mice were protected against bleomycin induced pulmonary fibrosis [94-96]. Mice were protected from bleomycin-induced lung fibrosis when exogenous SMAD7, an inhibitor of TGF-β signaling was administered [97]. Also, administration of exogenous TGF-β induced EMT in rat alveolar Type II cells, which was blocked by adenoviral-induced SMAD7 [98].

#### 1.2.5.2 Wnt signaling pathway

The best characterized Wnt signaling pathway is the β-catenin-dependent, or canonical, Wnt signaling pathway [99, 100]. In the absence of active Wnt ligands, β-catenin is constitutively

phosphorylated by its interaction with axin, adenomatosis polyposis coli (APC), and glycogen synthase kinase (Gsk-3β), and subsequently degraded. In the presence of Wnt ligands, two distinct membrane receptors, the frizzled (Fzd) or the low density lipoprotein receptor-related proteins (Lrp) 5 and 6, are activated upon ligand binding. This leads to phosphorylation of Lrp6 by Gsk-3β and casein kinase γ in its cytoplasmic region, which leads to the recruitment of axin. Subsequently, β-catenin phosphorylation is attenuated, its degradation inhibited, and accumulated β-catenin undergoes nuclear translocation, where it regulates target gene expression through interaction with members of the T-cell-specific transcription factor/lymphoid enhancer-binding factor (Tcf/Lef) family.

In IPF, Chilosi *et al*. [101] showed that nuclear β-catenin immunoreactivity localized to proliferative bronchiolar lesions and fibroblastic foci. β-catenin signaling can play a role in experimental EMT [101] suggesting that the aberrant nuclearization of β-catenin in bronchiolar lesions could promote EMT in the diseased lung. Matrix metalloproteinase-7 (matrilysin) is an important target gene of β-catenin [102]. Microarray screens have also revealed an increased expression of Wnt target genes, such as MMP7, or secreted frizzled-related protein (Sfrp) 2 in IPF [8, 12, 103]. Konigshoff *et al*. [104] demonstrate that the WNT/β-catenin signaling pathway is activated in the epithelium during lung fibrosis. The WNT target gene, WNT1-inducible signaling protein 1 (WISP1), was highly upregulated in experimental and idiopathic lung fibrosis.

## 1.3 EPITHELIAL-MESENCHYMAL TRANSITION

Epithelial mesenchymal transition is a process in which a polarized epithelial cell undergoes multiple changes which cause it to assume a mesenchymal cell phenotype, increased migratory capacity, resistance to apoptosis and increased production of extracellular matrix components [105]. EMT is said to be complete when the underlying basement membrane is degraded and the mesenchymal cell migrates away from the original epithelial layer. Many molecular processes like expression of cell-surface proteins, activation of certain transcription factors, reorganization of cytoskeletal proteins, production of extracellular matrix degrading enzymes and expression of certain microRNAs are initiated during EMT. EMT is seen during embryogenesis, organ development, wound healing, organ fibrosis and cancer. Immune privilege might be necessary for EMT associated with development but inflammation and epigenetics is necessary for fibrosis and carcinogenesis.

EMT has been characterized into three functional groups in a recent meeting in 2007 in Poland and subsequently in 2008 at Cold Spring Harbor Laboratories [106-109].

**Type 1:** During development, EMT plays a critical role in generating the first set of mesenchymal cells known as the primary mesenchyme. Subsequently, as diverse types of tissues are formed, the primary mesenchyme gives rise to secondary epithelia by a reversal of the process i.e. by mesenchymal epithelial transition.

**Type 2:** This EMT is a part of a repair process in which fibroblasts are formed to repair the tissue following injury or inflammation. This ceases once repair is achieved and the cause is removed. But in the presence of continued injury or inflammation, type 2 EMT continue the reparative process which ultimately leads to organ destruction by fibrosis.

**Type 3:** This occurs in epithelial cells which differ genetically and epigenetically from untransformed epithelial cells. These changes mainly affect oncogenes and tumor suppressors. The cells generated by type 3 EMT have the capacity to invade into the surrounding tissues, enter the blood circulation and ultimately metastasize into distant tissues. These metastatic nodules have secondary epithelia suggesting the capability of reversal of the EMT process.

While the three classes of EMT are distinct biological processes, a common set of elements seem to underlie these seemingly diverse programs [106-108]. Type 2 EMT shall be discussed in greater details as it is relevant to the topic being studied.

Type 2 EMT is found to be associated with fibrosis of the kidney, lung, liver and intestine. It is mediated by inflammatory cells and fibroblasts that release various inflammatory signals and components of the extracellular matrix such as collagens, laminins and elastins. Fibroblast specific protein 1 (FSP1), alpha smooth muscle actin, desmin, discoidin domain receptor tyrosine kinase 2 (DDR2) and collagen 1 are markers used to characterize mesenchymal cells produced by EMT [107]. Cells undergoing the process of EMT express these mesenchymal markers along with the epithelial markers cytokeratin, E-cadherin and zona occludens. EMT in the kidney has been studied more extensively than in the lung. Inflammatory injury to the mouse kidney results in recruitment of macrophages and activated resident fibroblasts that accumulate at the site of injury and release growth factors such as TGF-β, PDGF, EGF and FGF2 [110]. These cells also release chemokines and matrix metalloproteases (MMPs) like MMP2, MMP3 and MMP9. Contact of epithelial cells with the molecules leads to degradation of the basement membrane [110] and subsequently the epithelial cells migrate towards the interstitium under the gradient of growth factors and other chemoattractants. Fibroblasts produced by EMT express fibroblast-specific protein 1 which is regulated by a promoter element called fibroblast

transcription site-1 (FTS-1). The proteins CArG box-binding factor-A (CBF-A) and KRAB-associated protein 1 (KAP-1) bind this site. The FTS-1 site is also present in promoters of *Twist, Snai1, E-cadherin, β-catenin, ZO-1, vimentin, α-smooth muscle actin*. Venkov *et al*. showed that the formation of the CBF-A/KAP-1/FTS-1 complex is sufficient for the induction of FSP1 and a novel proximal activator of EMT [111].

TGF-β has been to shown to elicit EMT through HMGA2 [112]. HMGA2 (High Mobility Group AT-hook 2) or HMGI-C is a part of a family of nuclear factors that bind AT-rich DNA sequences in the minor groove and contribute to transcriptional regulation by altering the chromatin structure and organizing nucleoprotein complexes such as enhanceosomes [113-115]. Thuault et al. [112] showed that TGF-β directly targets HMGA2 through the SMAD transcription factors, mainly SMAD4 thereby increasing HMGA2 transcription.

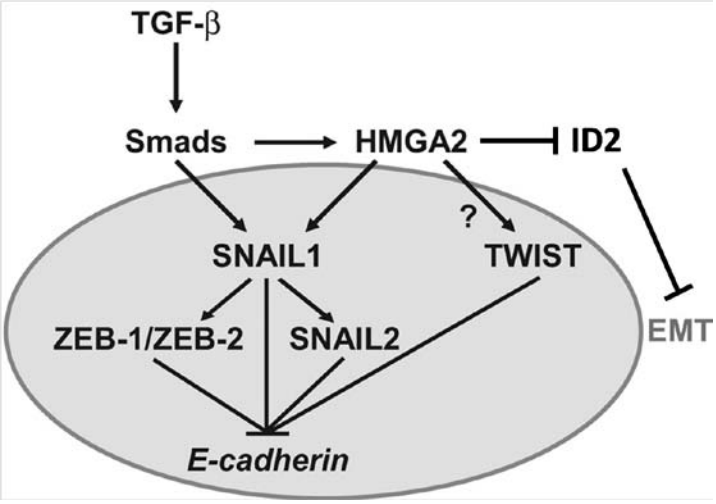


**Figure 2. Mechanistic model of EMT.**

An important event in EMT is the loss of E-cadherin which maintains cell-cell adhesion. SNAI1, SNAI2, ZEB1, ZEB2, TWIST, and E47 have all been identified as transcriptional repressors of E-cadherin [116]. HMGA2 regulates *Snai1, Snai2, Twist and Id2*, all key players of

EMT. TGF-β, through HMGA2, increases the expression of *Snai1, Snai 2 and Twist* but decreases that of *Id2.* The AT-hook domains of HMGA2 bind to the *Snai1* promoter DNA and also interact with the MH1 and MH2 domains of SMADs, leading to transcriptional activation of *Snai1* gene [117]. Snai1 regulates the expression of Snai2, ZEB1 and ZEB2 but not Twist. Id2 and Id3 form complexes with basic helix-loop-helix transcription factors such as E47 and inhibit the process of EMT [118, 119].

### 1.3.1 MicroRNAs and EMT

Recently, microRNAs have been shown to be a part of the processes involved in EMT. The microRNAs miR-200 and miR-205 inhibit the repressors of E-cadherin expression, ZEB1 and ZEB2 and help to maintain the epithelial cell phenotype [120-123]. This has been demonstrated in breast cancer. These miRNAs can hence be classified as tumor suppressors. In contrast, miR-21 [124, 125], mir-155 [126] and the miR-17~92 cluster [127] are upregulated in many cancers and facilitate TGF-β-induced EMT. MiR-21 is found in TGF-β-induced EMT in human keratinocytes, a model of epithelial cell plasticity for epidermal injury and skin carcinogenesis [128]. MiR-21 is abundantly expressed and associated with carcinogenesis. It targeted two tumor suppressors, tropomyosin 1 (TPM1) and programmed cell death-4 (*PDCD4*) to modulate the cell proliferation, microfilament organization, and anchorage-independent growth [129, 130]. The knockdown of miR-155 suppressed TGF-β-induced epithelial-mesenchymal transition (EMT) and tight junction dissolution, as well as cell migration and invasion. Further, the ectopic expression of miR-155 reduced its target RhoA, and disrupted tight junction formation [126]. Pottier *et al*. demonstrated that miR-155 targeted keratinocyte growth factor and the levels of miR-155 correlated with the degree of lung fibrosis in a mouse model [131].

### 1.3.2 Mesenchymal epithelial transition (MET)

The reverse process of EMT is MET in which the mesenchymal cells obtain epithelial cell characteristics. MET is seen during organ development when the mesenchymal cells generated as a result of EMT subsequently generate secondary epithelia. In tumors, the migratory cancer cells generate secondary metastatic nodules which exhibit an epithelial phenotype. Korpal *et al*. demonstrated that overexpression of the miR-200 family members either individually or as clusters in NMuMG cells hindered EMT by enhancing E-cadherin expression through direct targeting of *ZEB1* and *ZEB2* [121].

## 1.4 SMALL RNAS

At least three classes of small RNAs are encoded in the human genome, based on their biogenesis mechanism and the type of Argonaute protein involved: microRNAs (miRNAs), endo genous small interfering RNAs (endo‑siRNAs or esiRNAs) and Piwi‑interacting RNAs (piRNAs). MicroRNAs are expressed in all cell types whereas endo-siRNAs and piRNAs are expressed mainly in germ cells and contribute to germline development [132].

### 1.4.1 MicroRNAs

MicroRNAs were first discovered in C. *elegans* [133-138]. They are single-stranded RNAs of about 18-24 nucleotides in length processed from endogenous hairpin-shaped transcripts. MiRNAs are present within the introns of genes (intronic miRNAs) or may be in between genes

(intergenic). They are transcribed by either RNA polymerase II [139] or RNA polymerase III [140] into primary miRNA transcripts (pri-miRNA). These pri-miRNAs have a cap and a poly A tail which are hallmarks of polymerase II transcription. Lee *et al.* showed that their transcription is sensitive to treatment with the polymerase II inhibitor α-amanitin, and polymerase II binds to promoter sequences upstream of the miR-23a/miR-27a/miR-24-2 cluster [139]. In contrast, miRNAs encoded by the largest human miRNA cluster, C19MC, are transcribed by polymerase III [140]. Expression of selected miRNAs is under the control of transcription factors, for example c-Myc or p53 [141, 142], or depends on the methylation of their promoter sequences [143]. In addition, it has been shown that each miRNA located in the same genomic cluster can be transcribed and regulated independently. At present the microRNA database (microrna.sanger.ac.uk) contains 721 microRNAs.

MiRNA biogenesis [144, 145] takes place in the presence of two RNase enzymes, Drosha and Dicer. Both proteins have two tandem RNase III domains and a double-stranded RNA-binding domain (dsRBD). At the first step of miRNA biogenesis, the primary transcript which is generated upon RNA polymerase II transcription is cleaved at the stem of the hairpin structure by an RNase III-type protein Drosha to release the precursor form (pre-miRNA). Drosha acts in the presence of a cofactor DiGeorge syndrome critical region 8 (DGCR8) in humans and Pasha in *Drosophila melanogaster* and *Caenorhabditis elegans.* Drosha and DGCR8 together form a large complex called the Microprocessor complex which is ~650 kDa in humans. A pri-miRNA normally has a stem of about 33 bp, a terminal loop and flanking single stranded segments. DGCR8 interacts with these segments and the stem and assists Drosha in cleaving the transcript at ~ 11 bp away from the ssRNA-dsRNA junction. Two RNase III domains interact with each other to form a dimer. The first cuts the 3` strand whereas the second cuts the 5` strand forming a

2 nucleotide 3` overhang. The pre-miRNAs are transported to the cytoplasm in the presence of exportin 5 alongwith the cofactor Ran-GTPAse. Exportin 5 recognizes the >14bp dsRNA stem and the short 3` overhangs on either side. In the cytoplasm, the pre-miRNAs are cleaved by Dicer near their terminal loop to release ~22 nt miRNA duplexes. Dicer interacts with TAR RNA-binding protein (TRBP) and PACT which contribute to the formation of the RNA-induced silencing complex (RISC complex) along with Argonaute (Ago). The miRNA duplex is loaded onto and Ago protein to form the RISC. One strand remains as the mature miRNA (guide strand or miRNA) whereas the other strand (passenger strand or miRNA *) is degraded. Generally the strand with relatively unstable base pairs at the 5` end forms the mature miRNA. Some hairpins produce miRNAs from both strands.

For intronic miRNAs, cropping by Drosha and intron splicing are highly co-ordinated processes. Drosha processing takes place after the transcript is bound to the spliceosome complex but before the intron is spliced out. Sometimes, small RNAs are embedded in short introns and hence do not need Drosha for their processing. Following splicing, the intron forms a hairpin-shaped structure which is the precursor miRNA. Precursors formed in this manner are called mirtrons.

### 1.4.2 Let-7 family of microRNAs

The lethal-7 (let-7) gene was initially discovered as an essential developmental gene in C. elegans [136] and as one of the first miRNAs. The let-7 family of miRNAs is often present in multiple copies [146] in a genome and is highly conserved across species [147].

**Table 1. let-7 family in humans.**

| let-7 member | chromosome | strand | position | cluster |
|---|---|---|---|---|
| let-7a-1 | 9 | + | intergenic | let-7f-1, let-7d |
| let-7a-2 | 11 | - | intergenic | miR-100 |
| let-7a-3 | 22 | + | intergenic | let-7b |
| let-7b | 22 | + | intergenic | let-7a-3 |
| let-7c | 21 | + | intronic (C21orf34) | miR-99a |
| let-7d | 9 | + | intergenic | let-7f-1, let-7a-1 |
| let-7e | 19 | + | intergenic | miR-99b, miR-125a |
| let-7f-1 | 9 | + | intergenic | let-7a-1, let-7d |
| let-7f-2 | X | - | intronic(HUWE1) | miR-98 |
| let-7g | 3 | - | intronic(WDR82) | - |
| let-7i | 12 | + | intergenic | - |

Biological functions for let-7 include the regulation of stem-cell differentiation in C. *elegans* [136], neuromusculature development and adult behaviors in flies [148, 149], limb development in mouse [150], and cell proliferation and differentiation [148, 151-154]. Many let-7-family members function as tumor suppressors in a variety of cancers [155]. Whereas let-7-family of miRNAs have a distinct temporal pattern of expression in vertebrate development [152, 156, 157], a direct role for let-7 in vertebrate development has not been shown due to the difficulty associated with knocking out multiple let-7-family members in the same animal and the possible redundancy associated with such large families. In another study, let-7 was found to be expressed in breast-stem-cell progenitors as they differentiate [158]. In addition, reduced

expression of multiple let-7 members have been found to be associated with human cancers [155] and with cancer stem cells [151], leading to the strong suggestion that, as in C. *elegans*, let-7 genes function to promote terminal differentiation in development and function as tumor suppressors.

In vertebrates, the let-7 family has many more members than in C. *elegans* and D. *melanogaster* [133], including multiple forms that seem to be modified post-transcriptionally [159]. Interestingly, not only are the sequences and timing of expression of let-7 and many of its family members conserved across species [133, 147] but the genomic organization and clustering of miRNAs for many of the let-7 members is also conserved [160]. The selective pressure to conserve these clusters further underscores the importance of these genes and the need to maintain their correct expression patterns both spatially and temporally. In higher organisms, the levels of let-7 rise during embryogenesis [150], and pri-let-7a and pri-let-7e and mature let-7a, let-7c and let-7e are upregulated during mouse brain development [152]. Recent studies have found that a homolog of one of the C. *elegans* heterochronic genes, LIN28, is directly involved in the post-transcriptional regulation of the let-7 family of miRNAs in mammalian cells [161, 162]. LIN28 binds to the loop structure of what will become the precursor hairpin and prevents Drosha processing of pri-let-7 in the nucleus [161]. LIN28 also regulates the subsequent step by preventing the pre-let-7 from being turned into mature let-7 too early by binding to the pre-let-7 stem and preventing Dicer processing in the cytoplasm [163]. Lin28 interacts with pre-let-7 and mediates the terminal uridylation of pre-let-7 [164]. The uridylated pre-let-7 is resistant to Dicer processing due to its elongated tail and susceptible to degradation.

# 2.0 MATERIALS AND METHODS

## 2.1 SAMPLE COLLECTION

Lung tissue samples for microarray analysis were obtained through the University of Pittsburgh Health Sciences Tissue Bank as previously described [6, 7]. 10 samples were obtained from surgical remnants of biopsies or lungs explanted from patients with IPF who underwent pulmonary transplant and 10 control normal lung tissues obtained from the disease free margins with normal histology of lung cancer resection specimens. The morphologic diagnosis of IPF was based on typical microscopic findings consistent with usual interstitial pneumonia [165]. All patients fulfilled the diagnostic criteria for IPF outlined by the American Thoracic Society and European Respiratory Society [3]. All studies were approved by the Institutional Review Board at the University of Pittsburgh.

## 2.2 CELL CULTURE

A549 cells (CCL-185, American Type Culture Collection, Manassas, VA) and RLE-6TN cells (CRL-2300, ATCC) were grown in F12K medium (Invitrogen, Carlsbad, CA) with 2 mM L-glutamine and 10% fetal bovine serum. Primary normal bronchial epithelial cells (NHBE) (Lonza, Switzerland) were grown with the basal medium and BulletKit supplied by the company.

Cells were incubated at 37 °C in a humidified chamber supplemented with 5% $CO_2$. All experiments were done in 80% confluent cells. Before TGF-β, cells were serum starved overnight and treated 3 ng/ml TGF-β (R&D, Minneapolis, MN)

## 2.3 RNA ISOLATION

Total RNA from tissues and cells was isolated using the miRNeasy Mini kit (Qiagen, Valencia, CA) according to the manufacturer's instructions. The quantity of the RNA was determined by optical density, measured at 260nm by Nanodrop spectrophotometer. RNA quality was measured using the RNA 6000 Nano kit and the small RNA kit on the Agilent Bioanalyzer 2100.

## 2.4 MICROARRAYS

MicroRNA profiling was carried out using the Agilent Human microRNA Microarray. These microarrays have an 8 x 15K design with 470 microRNAs based on Release 9.1 of Sanger miRBASE. The manufacturer's instructions were followed in the labeling and hybridization of the RNA. Briefly, 100 ng of total RNA was dephosphorylated using calf intestine alkaline phosphatase (GE Healthcare, Piscataway, NJ), denatured with DMSO, and labeled with pCp-Cy3 using T4 RNA ligase (New England Biolabs, Ipswich, MA) at 16°C for 2h. The labeled RNA was purified using Micro Bio-spin 6 columns and hybridized onto the Agilent microRNA microarrays at 55°C for 20h. The arrays were washed with Gene Expression Wash Buffers 1 and 2 (Agilent) and scanned using the Agilent Microarray Scanner. The scanned images were

processed by Agilent's Feature Extraction software version 9.5.3. The gene expression microarrays have been previously described [13]. Briefly, lung samples were lysed in ice cold Trizol and total RNA was extracted and used as a template for double stranded cDNA synthesis. Labeling was performed using the Agilent Low RNA Input Linear Amplification Kit PLUS, (One-Color) (Agilent Technologies, Santa Clara, CA). Briefly, double stranded cDNA synthesis was performed using an oligo(dT) primer containing a T7 RNA polymerase promoter site. The cDNA was used as a template to generate Cy3 labeled cRNA that was used for hybridization. After purification and fragmentation aliquots of each sample were hybridized to Agilent Whole Human Genome 4 X 44K multi pack arrays (Agilent Technologies, Santa Clara, CA). After hybridization, each array was sequentially washed and scanned (Agilent DNA microarray scanner). Data files were normalized using cyclic LOESS. Differentially expressed genes were identified using Significant Analysis of Microarrays (SAM).

## 2.5 STATISTICAL ANALYSIS

MicroRNA microarray data was log2 transformed, normalized to the mean of each array and a Wilcoxon rank-sum test was used to identify those microRNAs that were differentially expressed (p-value < 0.05) between IPF and control lungs; each microRNA has 3-4 unique probes on the array. Only microRNAs whose mean values for each probes had an expression value >95% of the negative controls in at least one condition were considered for statistical analysis. Data visualization was accomplished using Genomica (http://genomica.weizmann.ac.il) [166] and Spotfire Decision Site 8.0 (Spotfire Inc., Göteborg, Sweden, http://spotfire.tibco.com). For qRT-PCR, statistical significance was determined by Student's t-test using $p<0.05$. *In s itu*

hybridizations were analyzed by student t-test and Mann-Whitney test to compare let-7d positive AECs/mm2 between IPF and control lung samples.

## 2.6 QUANTITATIVE RT-PCR

TaqMan MicroRNA assays (ABI, Foster City, CA) were used to determine the relative expression levels of microRNAs. For RT reactions, 50 ng of total RNA was used in each 15 µl reaction. The conditions for the RT reaction were: 16 °C for 30 min; 42 °C for 30 min; 85 °C for 5 min; and then held on 4 °C. The cDNA was diluted 1:14 and 1.33 µl of the diluted cDNA was used with the TaqMan primers in the PCR reaction. The conditions for the PCR were: 95 °C for 10 min followed by 40 cycles of 95 °C for 15 s and 60 °C for 1 min in the ABI 7300 real-time PCR system. The results were analyzed by the ΔΔCt method using RNU43 control RNA for normalizing human microRNAs and snoRNA55 for mouse microRNAs. Fold change was calculated taking the mean of the controls as the baseline. TaqMan gene expression assays (ABI) were used to determine the relative expression levels of HMGA2, CDH2, VIM, ACTA2, CDH1, ZO1 and COL1A. 500 ng of RNA was reverse transcribed using the SuperScript First-Strand Synthesis System for RT-PCR (Invitrogen) in a total reaction volume of 20 µl, the cDNA diluted 1:5 and 3 µl of this cDNA was used in a total volume of 31 µl for the PCR. PCR conditions were as follows: 12 min at 95°C, followed by 40 cycles with 15 s at 95°C and 1 min at 60°C in the ABI 7300 real-time PCR system. The results were analyzed by the ΔΔCt method and GUSB was used for normalization. Fold change was calculated taking the mean of the controls as the baseline.

## 2.7 MICRORNA PROMOTER ANALYSIS

Genomic coordinates of all differentially expressed microRNAs between IPF and control lungs and the coordinates of their murine orthologues were obtained from the UCSC Genome Browser [167]. The 1kb sequence upstream of the intergenic microRNAs and the 1kb sequence upstream of the host gene for the intronic microRNAs were collected. The host gene promoter sequence was used for intronic microRNAs because previous reports have shown that the microRNA and host gene are co-transcribed and share the same promoter region [168]. SMAD3 and SMAD4 binding site prediction was carried out with the FOOTER algorithm using default parameters [169].

## 2.8 CHROMATIN IMMUNOPRECIPITATION

The ChIP protocol was performed according to the published protocol from the Young laboratory [170]. A549 cells were grown to $5x10^7$ – $1x10^8$ cells per analysis condition. Cells were either untreated (control) or stimulated with 2 ng/mL TGF-β for 30 minutes. Chromatin cross-linking was performed by adding 1/10 volume of freshly prepared 11% formaldehyde solution for 15 minutes at room temperature. The cross-linking reaction was then quenched by adding 1/20 volume of 2.5M glycine. Cells were rinsed twice with PBS, collected with a silicon scraper, flash frozen in liquid nitrogen, and stored at -80°C until use. Upon thawing, cells were resuspended in a lysis buffer and sonicated at 4°C to solubilize cellular components and shear crosslinked chromatin. The cell lysate was incubated overnight at 4°C with 100 µl of Dynal Protein G magnetic beads that had been preincubated with 10 µg of either antiflag (mock IP) or

anti-SMAD3 antibodies (Millipore, Billerica, MA). Protein G magnetic beads were washed five times with RIPA buffer and one time with TE buffer containing 50 mM NaCl. Cross-linked promoter fragment/transcription factor complexes were eluted from the beads by heating at 65°C with vortexing at 2 minute intervals for 15 minutes. Crosslinking was reversed by incubation at 65°C overnight. Recovered promoter fragments were treated with RNaseA, proteinase K digestion, and purified by phenol:chloroform:isoamyl alcohol extraction/ethanol precipitation. Gene-specific PCR was performed on a portion of the purified recovered nucleic acid (35 cycles) to verify the presence of the upstream sequence of pre-hsa-let-7d. The primers used for gene specific PCR are: *let-7d forward*: 5' - CAC TTA AAC CCA GGA GGC AGA GGT T - 3' and *let-7d reverse*: 5' - ACC ACG TAT TAC TGG AGT CGC TGA - 3';

## 2.9 ELECTROMOBILITY SHIFT ASSAY

Cultured A549 lung alveolar epithelial carcinoma cells at 60-70% confluence were treated with 2 ng/mL recombinant human TGF$\beta_1$ (R&D Systems) for 60 minutes. Nuclear proteins were isolated using a standard rapid micropreparation technique described previously [171]. The supernatant was reserved and snap frozen in liquid nitrogen as the nuclear protein fraction. Nuclear extracts and recombinant full length SMAD3 protein (Santa Cruz Biotechnology, Santa Cruz, CA) were incubated with 5'-end Cyanine-5 labeled probe and/or non-labeled competitor oligonucleotide for 20 minutes at room temperature in a binding buffer consisting of 20% glycerol, 5 mM $MgCl_2$, 2.5 mM EDTA, 25 mM DTT, 200 mM NaCl, 50 mM Tris HCl pH 7.6, and 0.25 mg/mL poly(dI-dC). The complementary oligonucleotides (5' - GATAATTAAATGTTAAAAGTCAGC - 3', 5' - GCTGACTTTTAACATTTAATTATC

- 3') were synthesized by Integrated DNA Technologies (Coralville, IA), and consisted of a sequence upstream of the predicted SMAD3/let7d binding site (GGCTGAGTA). Additionally, a supershift assay was performed by incubating nuclear extract with 0.1 µl rabbit monoclonal antibody [EP568Y] to SMAD3 (Abcam, Cambridge, MA) or 1.0 µl mouse monoclonal [4A3] to peroxiredoxin 6 as a control (Abcam) prior to incubating with the target oligonucleotide. The protein/DNA complexes were run on a 6% native polyacrylamide gel and visualized on a Typhoon imaging and documentation system using Cyanine-5 dye excitation and fluorescence settings.

## 2.10 LUCIFERASE REPORTER ASSAYS

Luciferase assays were performed on A459 cells transfected with pGL4.17 (Promega, Madisson, WI) constructs containing -1600 to +87 base pair region of let-7d at the 5' end of the reporter gene. The eight base pair Smad3 site deletion (GCTGAGTA) plasmid was constructed using Quick Change mutagenesis kit (Stratagene, La Jolla, CA). The sequence of the deleted plasmid was confirmed by nucleotide sequencing from both strands. For TGF-β treatment A459 cells were grown to 80% confluence and stimulated for two hours at 10ng/ml. Reporter DNA was transfected using Lipofectamine 2000 (Invitrogen) at 1:1 ratio for 4h and cell growth continued for another 16h. Luciferase activity was determined using dual-reporter assay system (Promega).

## 2.11 TISSUE MICROARRAY (TMA) CONSTRUCTION

The tissue microarrays were previously described [172]. A total of 60 tissue samples consisting of 40 IPF and 20 control tissues derived from the normal part of lungs removed for benign lesions were snap-frozen and stored at -70°C. Specimens were fixed in cold-ethanol for 16 h and then embedded in paraffin. Hematoxylin and eosin (H&E) -stained sections were made from each block to define representative fibrotic and inflammatory lesion regions. Areas of interest were identified in H&E stained slides by a conventional microscope (Olympus BX-50). Tissue cylinders with a diameter of 1.5 mm were punched from selected areas of each "donor" block using a thin-wall stainless tube from a precision instrument (TMA-100, Chemicon, USA) and were transferred by a solid stainless stylet into defined array coordinates in a 45 * 20 mm new recipient paraffin block. The tissue microarray blocks were constructed in three copies (each containing one sample from a different region of all lesions). One sample was taken from the center and two samples from different peripheral areas. Ultimately, we constructed three tissue microarray blocks comprising of 80 tissue elements each. Each tissue element in the array was 1.5 mm in diameter and spacing between two adjacent elements was 0.1mm. After the TMA construction 5 μm sections for *in situ* hybridization analysis were cut from the "donor" blocks and were transferred to glass slides using an adhesive-coated tap sectioning system.

## 2.12 IN SITU HYBRIDIZATION

Lung tissues were obtained from the tissue bank of two different pathology centers (University Hospital of Alexandroupolis, Greece and the Veterans Administration Hospital, N.M.T.S,

Athens, Greece). The tissues were fixed in 10% formalin, paraffin-embedded and after the TMA construction samples were cut into 5 μm thick serial sections and were transferred to glass slides using an adhesive-coated tap sectioning system. The Rembrandt Universal RISH & AP Detection Kit (Invitrogen) was used for the in situ hybridization, with slight modifications. Briefly, the paraffin sections were dewaxed in xylene for 2 x 5 min, soaked in 100% ethanol. Then the paraffin sections were soaked in 75% ethanol and after in wash buffer solution so the tissue can retain its initial pH. The sections were then treated with proteolytic solution supplied in the kit for 20 min at 37°C. Excess proteolytic solution was discarded and the slides were dehydrated in 75%, 95% and 100% ethanol for 1 min each and then air-dried. Denaturation and hybridization was done overnight at 37°C with 20 nM 5`-digoxigenin labeled miRCURY LNA detection probe (Exiqon, Denmark) diluted in hybridization buffer (50% Formamide, 5xSSC, 0.1% Tween, 9.2mM citric acid for adjustment to pH 6, 50ug/ml heparin, 500ug/ml yeast RNA). The slides were washed in TBS buffer for 3 x 1 min. Slides were transferred onto a 37°C heating block or slide warmer and 2-3 drops of alkaline phosphatase conjugate were applied to each specimen. Slides were then incubated for 30 minutes at 37°C. Excess detection reagent was tapped off and slides were washed in TBS buffer. Slides were then soaked in three changes of TBS buffer for 1 minute each and then transferred into a container with distilled or deionized water and soaked for 1 additional minute. They were then taken out; excess of water was wiped off and dried around the edges using a lint-free cloth. Sections were then transferred onto a 37°C heating block and 2-3 drops of NBT/BCIP substrate were applied to each specimen. Then slides were incubated in the dark for 5-15 minutes at 37°C (color development was examined every 5 minutes with a light microscope) and removed from the heating block. They were then washed three times for 1 minute in changes of distilled or deionized water. The slides were

counterstained using Nuclear Fast Red. 2-3 drops of counterstain were applied to each slide (with hematoxylin for 10 sec) and rinsed in distilled water for 3 min. Slides were then incubated for 15 sec, excess of counterstain was tapped off and then they were washed briefly in distilled or deionized water. Images were acquired by using the high-resolution DUET, BioView scanning system for CISH, morphology applications.

## 2.13 CISH SEMIQUANTITATIVE IMAGE ANALYSIS

The number of let-7d positive alveolar epithelial cells (AECs)/$mm^2$ in 5 fields per case was counted by two independent pathologists - observers using the high-resolution DUET, BioView scanning system for CISH morphology and immunocytochemistry applications, at x100 magnification. Independent t-test and Mann-Whitney test were used to compare let-7d positive AECs/$mm^2$ between IPF and control lung samples.

## 2.14 IMMUNOHISTOCHEMISTRY

Tissue sections were treated as previously described [72]. Anti- HMGA2 rabbit polyclonal antibody (4 μg/ml) (Abcam) was applied and samples were incubated at 4°C overnight. A secondary biotinylated anti-immunoglobulin followed by horseradish peroxidase-conjugated streptavidin (BioGenex, San Ramon, CA) was used according to manufacturer's instructions. 3-amino-9-ethyl-carbazole (BioGenex) in acetate buffer containing 0.05% $H_2O_2$ was used as

substrate. The sections were counterstained with hematoxylin. The primary antibody was replaced by non-immune serum for negative control slides.

Mouse lung tissue was fixed and inflated with PROTOCOL SafeFix (Fisher Scientific, Waltham, MA). Tissue sections were deparaffinized and rehydrated using xylene and sequential ethanol rinses, endogenous peroxidase activity blocked with methanol and hydrogen peroxide, antigen retrieval done by heating the slides in sodium citrate buffer pH 6.0 at 95 °C for 30 min followed by blocking in 5% goat serum for 30 min. The sections were incubated with the appropriate antibody for 1 hour at room temperature. Following two 5 min washes in TBS, the sections were incubated in the secondary antibody for 30 min, washed twice for 5 min in TBS, incubated for 30 min with RTU Vectastain Elite ABC Reagent (Vector Laboratories), washed in TBS stained with DAB Substrate kit (Vector Laboratories) according to the manufacturer's instructions, counterstained with hematoxylin and mounted in Vectashield hardset mounting medium (Vector Laboratories). The number of ACTA2 positive alveolar epithelial cells (AECs) in 10 fields per slide was counted by two independent pathologists at x60 magnification. T-test was used to compare ACTA2 positive AECs between saline and antagomir-treated lung sections.

## 2.15 TRANSFECTION

A549 cells, RLE-6TN cells and NHBE cells were plated in 6-well plates at 50% confluence. A549 cells and RLE-6TN cells were plated in F12K medium containing 10% fetal bovine serum while NHBE cells were plated in the basal medium supplemented with the bullet kit supplied by Lonza. After the cells were adherent, the medium was changed to Opti-MEM I reduced serum medium (Invitrogen). Transfection of hsa-let-7d inhibitor, pre-let-7d and their corresponding

negative controls (Ambion, Austin, TX) was carried out at 50 nM using Lipofectamine 2000 (Invitrogen) according to the manufacturer's instructions. RNA was isolated 24h and 48h post transfection.

## 2.16 IMMUNOBLOTTING

Immunoblotting was used to detect the protein expression in RLE-6TN cells grown in 6-well plates were transfected either with the scrambled oligonucleotide or let-7d inhibitor. The cells were washed in ice-cold phosphate-buffered saline (PBS) and lysed at 4º C with a solution containing 50 mM Tris-HCl pH 7.4, 150 mM NaCl, 1mM PMSF, 1mM EDTA, 5µg/ml aprotinin, 5µg/ml leupeptin, 1% Triton x-100, 1% sodium deoxycholate and 0.1% SDS. The soluble cell lysate was centrifuged at 16000 x g for 15 min and the supernatant was transferred to a clean microcentrifuge tube. Protein concentrations were measured using the BCA Protein Assay Kit (Pierce, Rockford, IL). 10 µg of the lysate was resolved by sodium dodecyl sulfate polyacrylamide gel electrophoresis (SDS-PAGE) and transferred onto an Immobilon-P membrane (Millipore Corporation, Billerica, MA). After blocking with 3% bovine serum albumin for 1h, the membrane was incubated overnight with the desired antibody at 4º C. Following three 10 min washes with tris-buffered saline Tween-20 (TBST), the membranes were incubated with the appropriate secondary antibody for 1h at room temperature. Target proteins were observed using the Western Lightning Chemiluminescence Reagent Plus Kit (Perkin Elmer Life Sciences, Boston, MA) according to the manufacturer's instructions. Equal protein loading was assessed by stripping the membranes with 0.1M glycine, pH 2.0 and reprobing with

antibodies against β-actin (Sigma) or lamin A/C. Densitometric analysis was performed using the ImageJ software (National Institute of Health).

## 2.17 IMMUNOFLUORESCENCE

A549 cells were plated on cover slips. Cells were starved for 24 hours by the removal of serum and transfected with 50 nM anti-let7d for 48 hours. Cover slips were removed, and fixed in 2% paraformaldehyde (Sigma) for 40 minutes. Permeabilization of cells was carried out by using 0.1% Triton X in PBS for 40 minutes, with three washes in PBS each for five minutes followed by blocking with 0.3% BSA and 5% goat serum in PBS for 60 minutes, and incubated with anti-cytokeratin, anti-vimentin, anti-N-cadherin, or anti-alpha-smooth muscle actin (all from Abcam Inc., Cambridge, MA) in 0.5% BSA in PBS for 60 minutes. Following three washes with 0.5% BSA in PBS (5 minutes each), coverslips were incubated with the appropriate secondary antibody (Invitrogen, Carlsbad, CA) for one hour at 37°C. After staining, cover slips were washed with 0.1% Triton in PBS for 2 times 5 minutes each followed by three washes with PBS 5 minutes each. Coverslips were inverted onto slides and mounted in Vectashield anti-fade medium that contained DAPI for nuclei staining (Vector Laboratories, Burlingame, CA) to prevent photobleaching. Slides were examined using a Leica TCS-SP2 laser scanning confocal microscope equipped with appropriate lasers for simultaneous imaging of up to four fluorophores.

Lung tissue from mice was frozen into OCT blocks and sectioned. The frozen sections were fixed in ice cold acetone for 15 min. After washing the sections twice for 2 min each in PBS, avidin-biotin blocking was performed using the Avidin/Biotin Blocking kit (Vector

Laboratories) according to the manufacturer's instructions. The sections were blocked for 30 min in a blocking buffer consisting of 5% goat serum and 3% bovine serum albumin in PBS. The sections were then incubated in the desired primary antibody for 1h, washed for 5 min in PBS and incubated in the appropriate secondary antibody for 30 min. After washing for 5 min in PBS, the sections were incubated in Fluorescein Avidin DCS for 10 min followed by another wash of 5 min in PBS. This procedure was repeated for the second antibody but incubated with Texas Red Avidin DCS for 10 min. The nuclei were stained with 4'-6-Diamidino-2-phenylindole (DAPI) for 1 min, washed in PBS for 5 min and mounted using VECTASHIELD HardSet Mounting medium (Vector Laboratories). Slides were examined using an Olympus Fluoview 1000 confocal microscope equipped with appropriate lasers. Colocalization was quantified using MetaMorph software (Molecular Devices, CA).

## 2.18 SYNTHESIS OF ANTAGOMIR

The design of the let-7d antagomir was adapted from Krutzfeldt *et al* [173]. The single-stranded RNA 5` -aacuaugcaaccuacuaccucu- 3` was custom synthesized from Dharmacon, Lafayette, CO. The sequence of the oligonucleotide was complementary to that of mmu-let-7d. All bases had 2'-O-methyl modifications, the first two bases and the last four bases had phoshorothioate linkages and a cholesterol molecule was conjugated at the 3' end. The sequence of the scrambled control was 5` -aaccauguaaacuacuacaucu- 3`.

## 2.19 ANIMALS

6-12 week old C57BL/6 mice were purchased from the Jackson Laboratory and housed under pathogen-free conditions. The studies were approved by the Animal Care and Use Committee at the University of Pittsburgh. In the shorter protocol, 4 mice were treated either with 10 mg/kg body weight let-7d antagomir administered intratracheally in 50 µl or an equal volume of saline. In the extended protocol, mice were administered the antagomir on days 1, 2, 3, 8, 9, 10, 15, 16, 17 and sacrificed on day 18. Two control mice were administered the same volume of saline in each of the three groups. There were 7 mice in each group when the scrambled control was used.

## 2.20 BLEOMYCIN ADMINISTRATION

0.0375 U of bleomycin (Hospira, IL) was administered intratracheally in 50 µl of 0.9% saline. Mice were sacrificed after 14 days and RNA isolated from the lungs.

## 2.21 MASSON'S TRICHROME STAINING

Sections were stained as per the established protocol [174] by the University of Pittsburgh Transplantation Institute Core Facility. 10 images per slide were obtained. Airways and blood vessels were avoided so as to not introduce any bias in the quantitation. The total tissue per section was quantified as the area in pixels. The total blue stain was also measured as area in pixels. MetaMorph software (Molecular Devices) was used to perform the analysis.

# 3.0 RESULTS

## 3.1 MICRORNAS ARE DIFFERENTIALLY EXPRESSED IN IPF AND CONTROL LUNGS

Total RNA from 10 control and 10 IPF lungs was isolated, labeled with Cy3 dye and hybridized on Agilent microRNA microarrays. Fig. 3 shows the heatmap generated from the microRNA microarray data. Every column represents a patient and every row represents a microRNA. Yellow represents upregulated and purple represents downregulated microRNAs. Expression of the microRNAs showing no difference between the two groups being compared is grey. The heatmap on the left represents the global microRNA expression. The heatmap on the right represents statistically significant ($p$-value < 0.05) differentially expressed microRNAs. Let-7d, miR-30 family, miR-26 family and several members of the miR-17~92 cluster are downregulated in IPF. The entire microRNA microarray dataset has been deposited in the Gene Expression Omnibus (GSE13316).

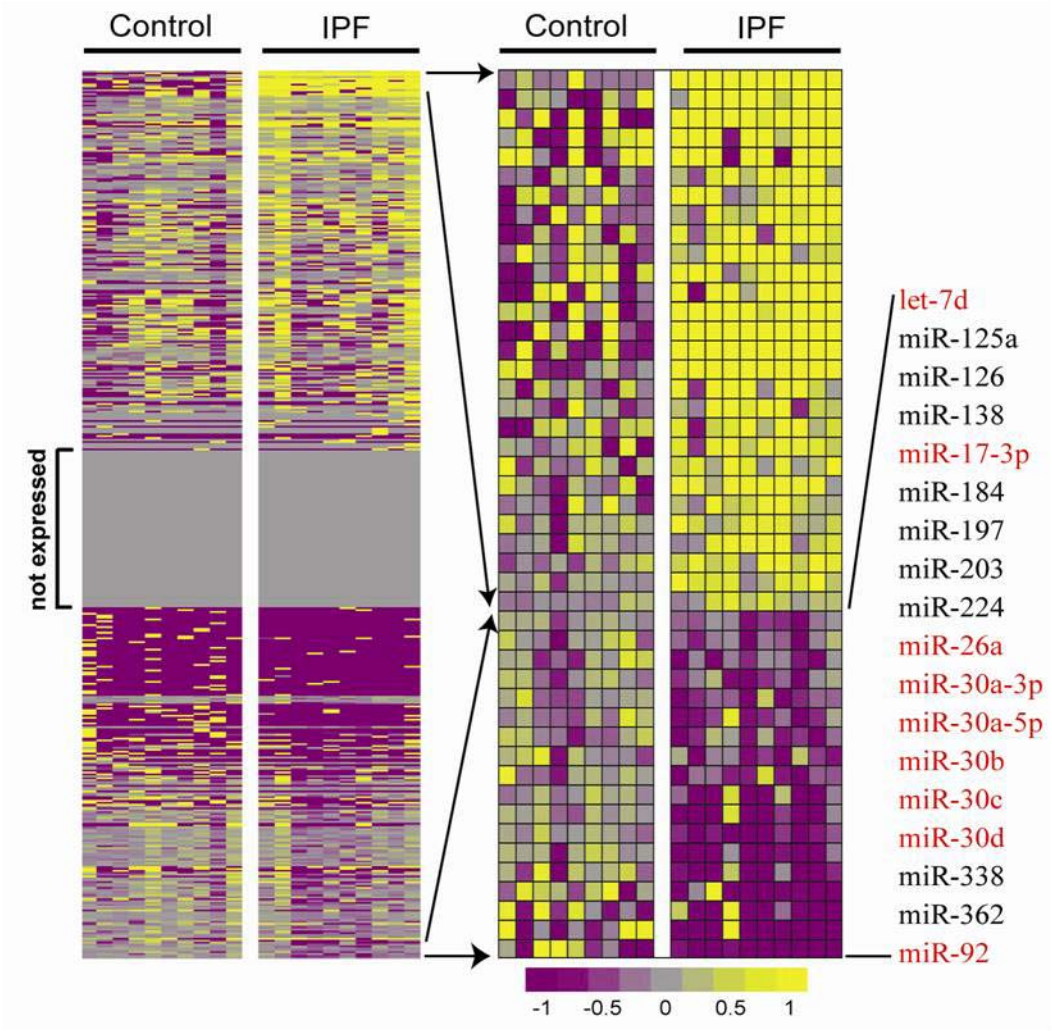


**Figure 3. microRNAs are differentially expressed in IPF.**

To validate our microarray results, we performed qRT-PCR of 14 microRNAs that significantly decreased according to our microarray data. The relative changes of microRNA expression assayed using microarray analysis and qRT-PCR were consistent. Validation of the microarray results confirmed that let-7d, miR-26 family, miR-30 family and the miR-17~92 cluster were indeed significantly ($p<0.05$) downregulated (Fig. 4).

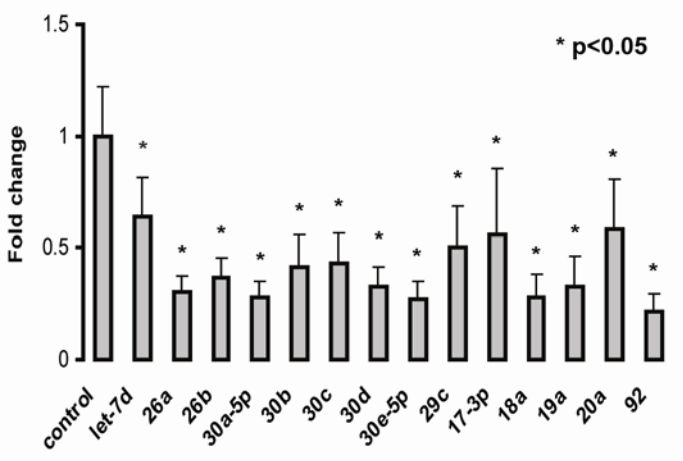


**Figure 4. qRT-PCR verification of the microarray results of reduced let-7d, miR-26 and miR-30 families and the miR-17~92 cluster in IPF.**

Though the bleomycin model cannot be promoted as an experimental equivalent of IPF, it is the most common method of inducing experimental pulmonary fibrosis. We assessed whether let-7d expression was similar in mice treated with bleomycin (Fig. 5). Let-7d expression is significantly decreased at day 14 post-bleomycin administration which falls within the "fibrotic phase".

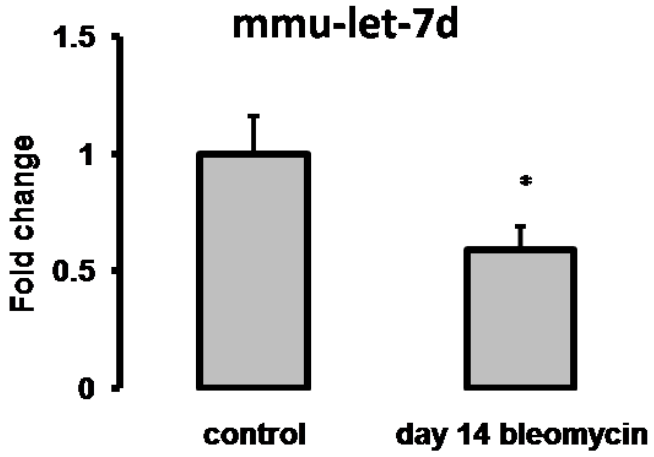


**Figure 5. let-7d expression in mice treated with bleomycin.**

Since the gene expression profile of IPF lungs is enriched with genes from developmental pathways [66], we quantified these validated down-regulated miRNAs in fetal lung tissue. Most of the microRNAs downregulated in IPF were also downregulated in fetal lung tissues as assessed by real-time PCR (Fig. 6). There were 10 tissue samples in each set. Yellow denotes an increase and purple denotes a decrease in expression.

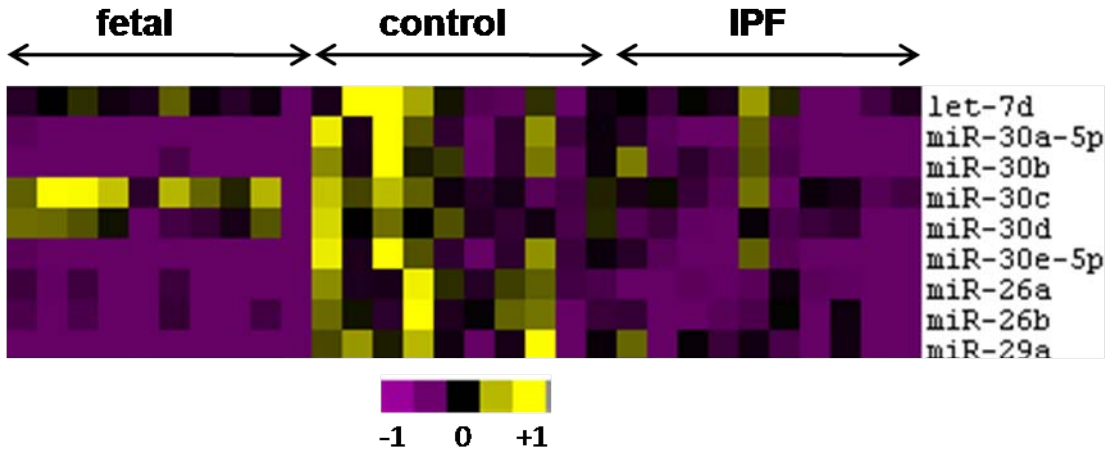


**Figure 6. MicroRNA expression in control, IPF and fetal tissues.**

It can be concluded that let-7d expression is decreased in IPF, fetal lungs and in the bleomycin model of lung fibrosis.

## 3.2 LET-7D IS REGULATED BY TGF-β

### 3.2.1 FOOTER algorithm predicts a SMAD3 binding site upstream of let-7d

MicroRNAs have certain similarities to protein coding genes. Most microRNAs are transcribed by RNA polymerase II [139], their immediate upstream regions are conserved across species,

and they have similar sequence features to protein coding genes in their core promoter regions [175]. These observations suggest that the transcriptional mechanism of miRNAs is similar to protein coding genes transcribed by RNA polymerase II. Since TGF-β is the main cytokine implicated in the pathogenesis of IPF and exerts its actions through the SMAD family of transcription factors, we determined whether any of the differentially expressed miRNAs had binding sites for SMAD proteins in their upstream regions. We used the FOOTER algorithm [169] for this purpose. FOOTER assigns a score to the motif taking into consideration the sequence conservation across different species and known binding sites from the TRANSFAC database.

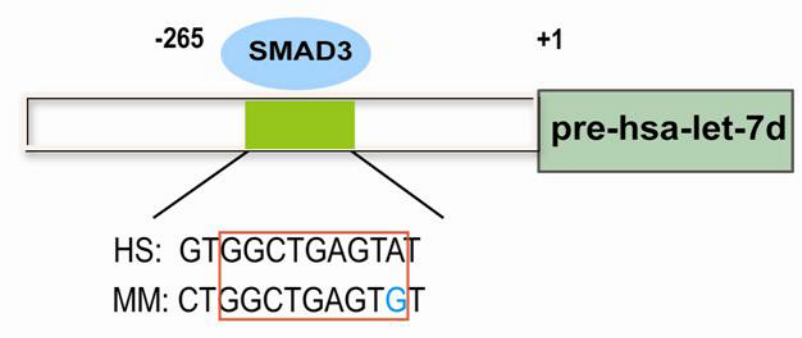


**Figure 7. Putative SMAD3 binding sites identified by the FOOTER algorithm.**

A SMAD3 binding site was computationally predicted at position -265 from pre-hsa-let-7d (Fig. 7) using FOOTER. In the figure, the human (HS) and mouse (MM) sequences are shown.

### 3.2.2 TGF-β downregulates let-7d *in vitro*

To determine whether TGF-β indeed affected the expression of let-7d, we stimulated A549 cells in culture with 3 ng/ml of recombinant TGF-β. The expression of hsa-let-7d was significantly

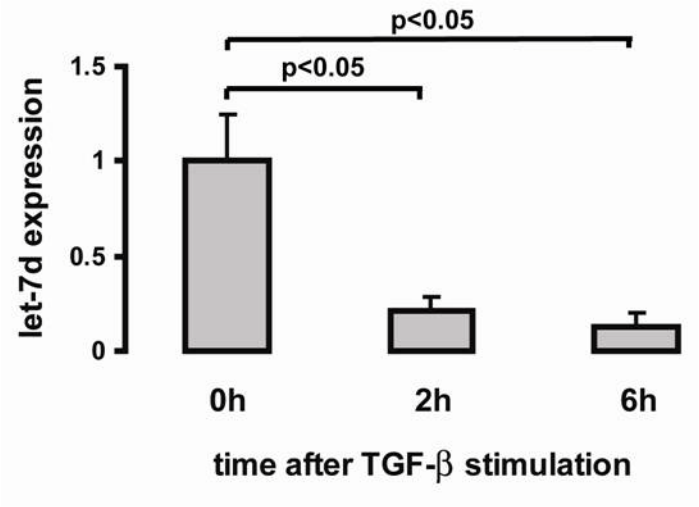


**Figure 8. Decreased expression of let-7d on stimulation of A549 cells with TGF-β**

reduced (85% decrease) at 2h and 6h post-stimulation (Fig. 8) demonstrating that TGF-β did suppress the expression of hsa-let-7d. The results represent an average expression ± S.D. of triplicate experiments. These results suggest that TGF-β alters the levels of let-7d either directly through binding of one of the SMAD transcription factors to the promoter of let-7d or indirectly by acting on an intervening molecule.

### 3.2.3 EMSA demonstrates interaction of SMAD3 with the predicted promoter of let-7d

To determine if SMAD3 had an affinity for this predicted binding site in the upstream region of let-7d, we performed an electrophoretic mobility shift assay (EMSA). Incubation of target DNA

with either recombinant SMAD3 protein (lanes 2, 3 and 4) or nuclear extract of A549 cells (lanes 5, 6 and 7) revealed distinct bands representing the binding of SMAD3 to the let-7d promoter sequence (Fig. 9). The intensity of these bands diminished in the presence of increasing

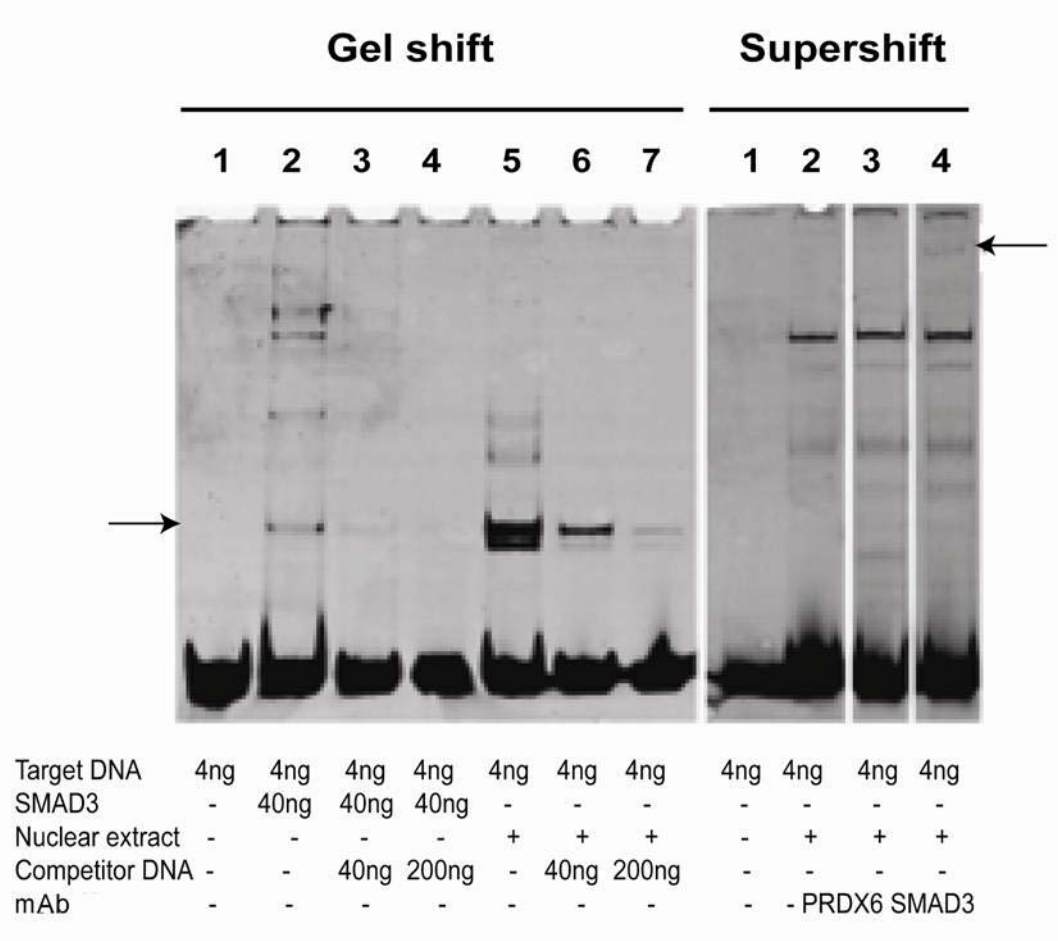


**Figure 9. EMSA demonstrates binding of SMAD3 at the predicted promoter of let-7d.**

concentrations of competitor DNA. A supershift was demonstrated by incubating the target DNA and nuclear extract in the presence of antibodies to SMAD3 and peroxiredoxin 6. The supershift band representing the DNA-protein-antibody complex was visible with SMAD3 antibody but not with the control peroxiredoxin 6 antibody. This proved that the SMAD3 binding was specific.

### 3.2.4 Chromatin immunoprecipitation demonstrates SMAD3 binding to the predicted promoter *in vivo*

SMAD3 ChIP revealed minimal binding of SMAD3 with the let-7d promoter at baseline (lane 1) (Fig. 10).


**Figure 10. SMAD3 ChIP assay revealed association with let-7d in A549 cells.**

A significant band was seen when a SMAD3 immunoprecipitation was performed on A549 cells following TGF-β stimulation (lane 2). Lane 3 demonstrates the binding in whole cell extract following TGF-β stimulation whereas lane 4 represents a mock immunoprecipitation in the presence of anti-Flag antibody.

### 3.2.5 SMAD3 is a transcription factor for let-7d

The promoter activity of the 5' region of let-7d was further analyzed using a luciferase reporter assay (Fig. 11). The 1687 base pair region (-1600 to +87) (p-let-7d-luc) and an 8 base pair

SMAD3 binding site deletion mutant (p-mlet-7d-luc) were PCR amplified and cloned into the 5' end of the luciferase gene. The reporter constructs and empty vector controls were transfected into A459 cells with and without TGF-β activation and luciferase activity measured.

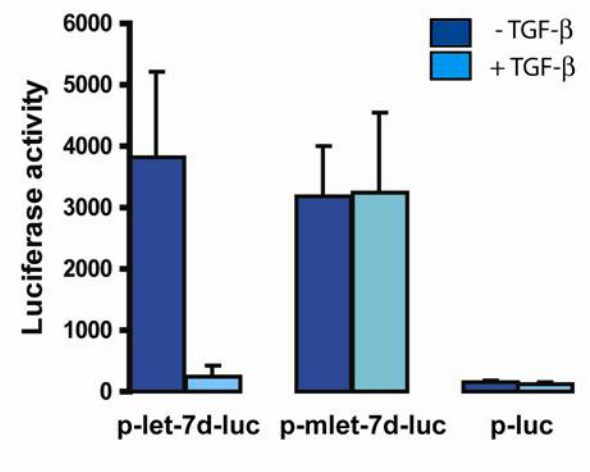


**Figure 11. Luciferase assay confirms promoter activity of the predicted SMAD3 binding site.**

The 1687 base pair region increased the average reporter activity by 25 fold showing that this region did have intrinsic promoter activity. Luciferase activity was reduced to less than 30% in TGF-β treated cells as compared to untreated controls. This TGF-β mediated inhibition of luciferase activity was eliminated when we used the 8 base pair SMAD3 binding site deletion mutant. The presented results are representative of at least three experiments. Hence we can conclude that SMAD3 is a transcription factor for let-7d and negatively regulates the expression of let-7d.

## 3.3 LET-7D AND MIR-30 ARE DOWNREGULATED IN IPF

TGF-β reduces the expression of let-7d by direct SMAD3 binding to the promoter of let-7d and there is abundant active TGF-β signaling in IPF. This explains our finding of decreased let-7d in IPF.

### 3.3.1 Microarray and real-time PCR demonstrate decreased let-7d and miR-30 family in IPF lungs

As mentioned earlier, microRNA microarrays on lung tissues of control subjects and IPF patients revealed down-regulation of let-7d and miR-30 family which was subsequently confirmed by real-time PCR (Fig. 3 and 4).

### 3.3.2 In situ hybridization localizes let-7d and miR-30 to alveolar epithelial cells

In order to determine the downstream effects of the decrease of these microRNAs in IPF, we initially wanted to localize them in the lung. We performed an *in situ* hybridization on tissue microarrays which had 40 IPF tissues and 20 control tissue sections. Staining for let-7d and miR-30e on lung tissues demonstrated abundant let-7d and miR-30e in control lung sections in comparison to IPF. They stained in alveolar epithelial cells (Fig. 12). Panels (i), (iii) and (v) are control lungs whereas panels (ii), (iv) and (vi) are IPF lungs.

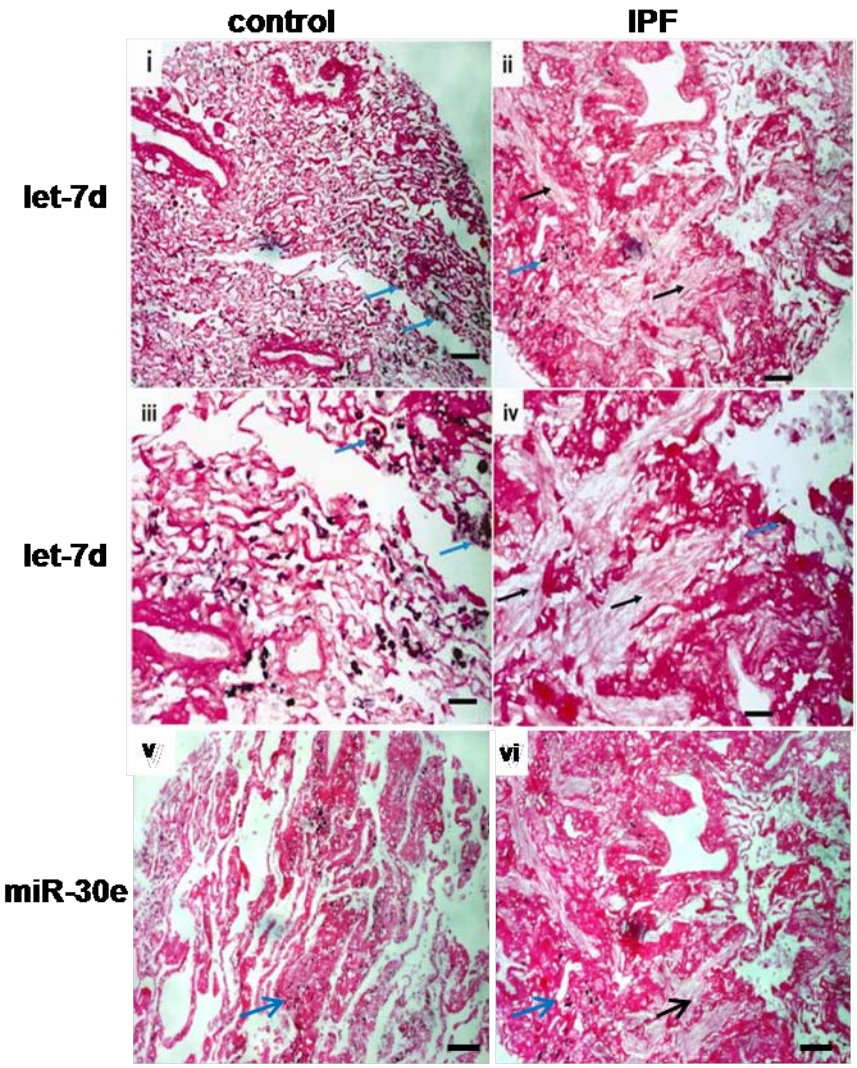


**Figure 12. Tissue microarray analysis reveals that let-7d and miR-30e localize within normal alveolar epithelium in control lungs and is nearly absent from fibrotic areas in IPF lungs.**

Let-7d is localized in alveolar epithelial cells of control lungs as evident by the black staining (blue arrows). The black arrows point to areas of dense fibrosis while blue arrows point to minimal staining in the immediate surrounding areas. It should be noted that in IPF tissues, let-7d and miR-30e does stain in the histologically normal areas but is absent in areas of fibrosis. Scale bars in panels (i) and (ii) denote 100 µm while those in (iii), (iv), (v) and (vi) represent 25 µm.

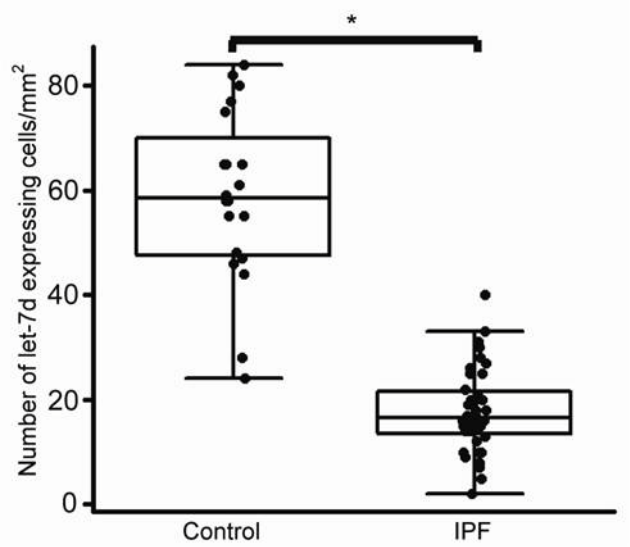


**Figure 13. Number of let-7d expressing cells/mm3 was significantly lower in IPF.**

The number of let-7d positive alveolar epithelial cells (AECs)/mm$^2$ in 5 fields per case was counted by two independent pathologists - observers using the high-resolution DUET, Bioview scanning system for CISH morphology and immunocytochemistry applications, at x100 magnification. Independent t-test and Mann-Whitney test were used to compare let-7d positive AECs/mm$^2$ between 40 IPF and 20 control lung samples. There was almost a three-fold reduction in let-7d positive cells in the IPF lungs (Fig. 13).

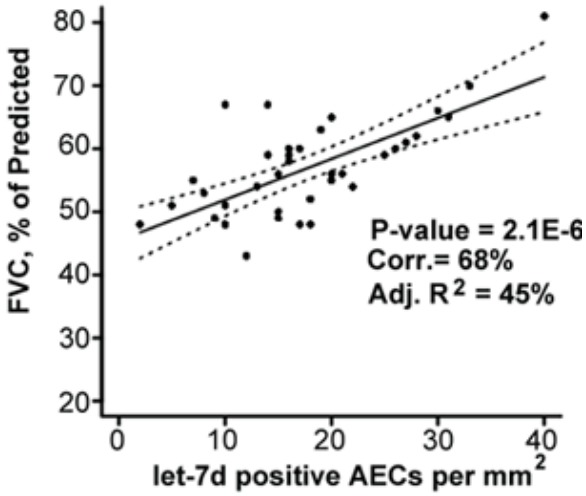


**Figure 14. Positive correlation of FVC and let-7d.**

Lung function studies of these patients show a positive correlation of number of let-7d stained cells to the forced vital capacity (FVC) (Fig. 14). FVC is commonly used to define severity and to follow the course of patients with IPF. FVC is believed to be a physiologic correlate of the extent of fibrosis. The detailed counts per patient with the corresponding FVC are included in Appendix B. This indicates that let-7d expression levels can possibly be used as a marker for disease progression.

## 3.4 HMGA2, A LET-7D TARGET IS UPREGULATED IN IPF

We found let-7d to be downregulated in IPF lungs and localized it to alveolar epithelial cells. In order to determine the mechanism by which this reduction in let-7d contributes to the pathogenesis of IPF, we looked for possible targets in the microRNA target database TargetScan (www.targetscan.org). HMGA2 and RAS were putative targets of interest. Both HMGA2 and RAS are proven direct targets of let-7 microRNAs [176, 177] and both have been shown to have a role in EMT in cancers [112, 117, 178]. We initially focused on HMGA2 because it has six let-7 complementary sites in its 3` UTR.

### 3.4.1 Microarray and real-time PCR demonstrate increased HMGA2 in IPF lungs

Gene expression microarrays on lung tissues of control subjects and IPF patients revealed up-regulation of HMGA2 which was subsequently confirmed by real-time PCR (Fig 15).

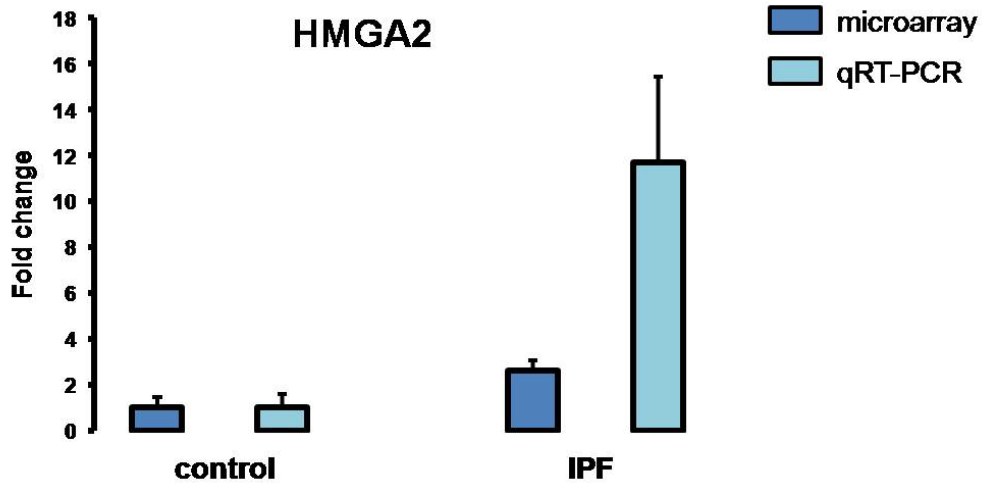


**Figure 15. HMGA2 is upregulated in IPF by microarray and qRT-PCR.**

HMGA2 was expected to be increased in IPF since the inhibition of let-7d on HMGA2 was decreased. Also, IPF lungs are characterized by a developmental gene signature [10, 11, 13, 66]. HMGA2 is a developmental gene. It is expressed early during embryogenesis and is silenced in adult tissue.

### 3.4.2 Immunohistochemistry localizes HMGA2 to alveolar epithelial cells in IPF lungs

Consistent with the results demonstrating downregulation of let-7d in IPF lungs, immunohistochemistry revealed expression of HMGA2 in alveolar epithelial cells and in some capillary endothelial cells of IPF lungs but not in control lungs.

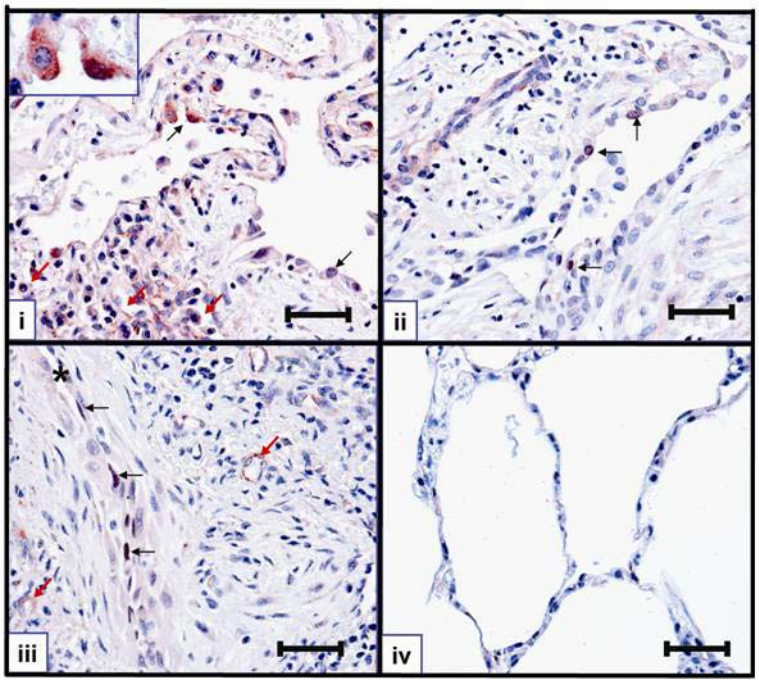


**Figure 16. Immunolocalization of HMGA2 in IPF and normal lungs.**

In Fig. 16 panels (i) and (ii) show two different IPF lungs demonstrating the immunoreactive protein primarily in alveolar epithelial cells, either in cytoplasm or nuclei (black arrows). The red arrows in (i) point to collapsed air spaces which are lined by HMGA2 positive epithelial cells. Panel (iii) shows nuclear staining of HMGA2 in elongated epithelial cells (asterisk indicates an alveolar space) and some fibroblast-like cells immersed in a fibroblastic focus. Positive endothelial cells are marked with red arrows. Normal lungs in panel (iv) were negative for HMGA2. The scale bars in all panels denote 100 µm.

## 3.5 INHIBITION OF LET-7D RESULTS IN INCREASED HMGA2 EXPRESSION

Let-7 microRNAs have been previously shown to downregulate HMGA2 [176], a mediator of TGF-β-induced EMT [112]. Considering that we found downregulation of let-7d and concomitant upregulation of HMGA2 in IPF lungs we explored whether TGF-β induced HMGA2 and whether let-7d was a regulator of HMGA2 expression in lung epithelial cell lines.

### 3.5.1 TGF-β induces HMGA2 expression

As mentioned ealier, stimulation of A549 cells by TGF-β caused a dramatic reduction in levels of let-7d at 2h and 6h post-stimulation. Since the let-7 family targets HMGA2 [176], we expected a corresponding increase in HMGA2. Stimulation of A549 cells by TGF-β did lead to a significant increase in HMGA2 ($p$<0.05) (Fig 17).

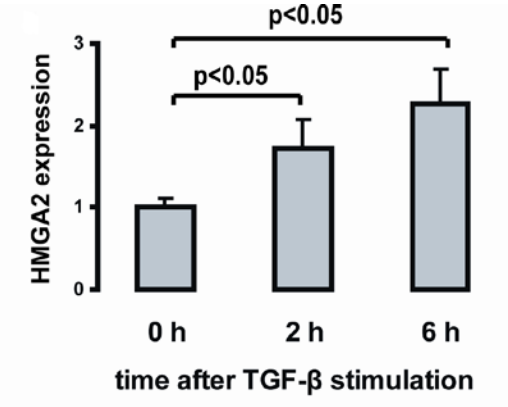


**Figure 17. TGF-β increases HMGA2 expression.**

### 3.5.2 HMGA2 is a target of let-7d in a lung epithelial cell line

The let-7 family was shown to target HMGA2 in a variety of cells but not in a lung epithelial cell line. Before determining the functional role of the increase in HMGA2 we verified that HMGA2 is targeted by let-7d also in a lung epithelial cell line. Transfection of A549 cells with a let-7d inhibitor for 24h and 48h led to a significant increase in HMGA2 at 24h that remained elevated at 48h.

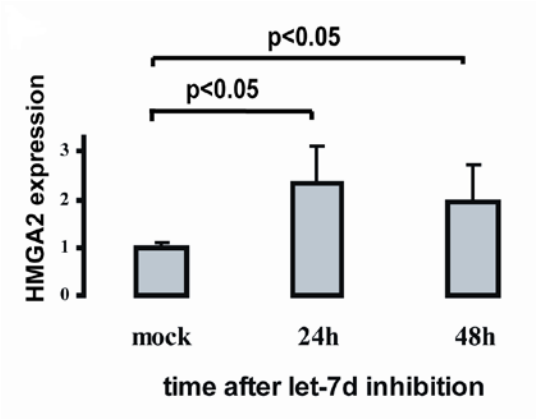


**Figure 18. Inhibition of let-7d causes an increase in HMGA2.**

### 3.5.3 let-7d prevents TGF-β induced increase in HMGA2

TGF-β reduces let-7d levels through SMAD3 and let-7d in turn reduces HMGA2. Thuault *et al*. [112] demonstrated that TGF-β also increases HMGA2 by direct binding of SMAD4 to the promoter of HMGA2. Overexpression of let-7d in RLE-6TN cells by transfection with pre-let-7d prevented the TGF-β induction of HMGA2.

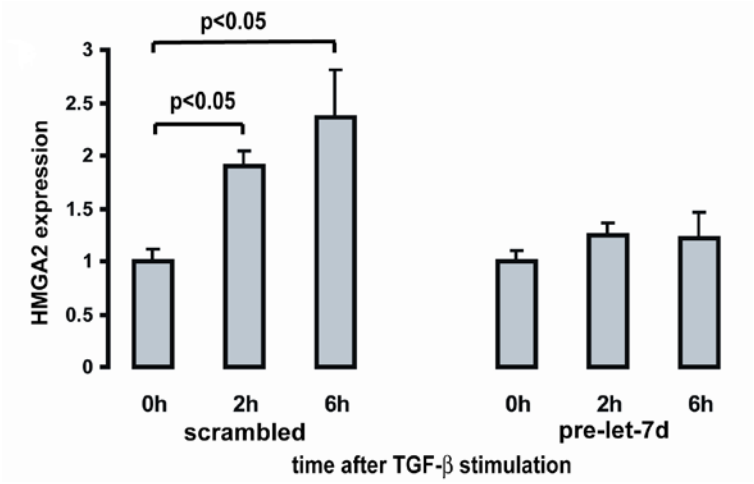


**Figure 19. let-7d prevents TGF-β-mediated increase in HMGA2.**

These results demonstrate that let-7d is a regulator of HMGA2 expression in lung epithelial cell lines and that the increase in HMGA2 after TGF-β stimulation is in part dependent on inhibition of let-7d by TGF-β.

## 3.6 INHIBITION OF LET-7D RESULTS IN EMT

Since let-7d targets HMGA2 a known mediator of TGF-β-induced EMT [112], we evaluated whether altering let-7d levels induces EMT *in vitro*.

### 3.6.1 Real time PCR demonstrates an increase in mesenchymal markers following inhibition of let-7d

We inhibited let-7d in A549 cell line, RLE-6TN cell line and primary normal human bronchial epithelial (NHBE) cells. Levels of the mesenchymal markers alpha-smooth muscle actin

(ACTA2), vimentin (VIM) and N-cadherin (CDH2) were measures at 48h post-transfection. All three markers were significantly increased in both A549 and RLE-6TN cell lines. VIM and ACTA2 increased but CDH2 remained unchanged in primary NHBE cells.

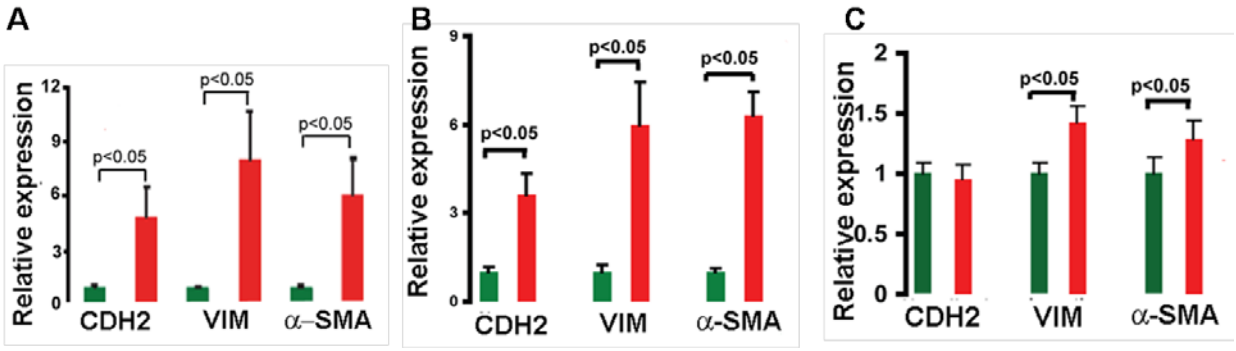


**Figure 20. Inhibition of let-7d results in increased mesenchymal markers in (A) A549 cell line, (B) RLE-6TN cell line and (C) NHBE primary cells.**

### 3.6.2 Immunofluorescence and immunoblotting reveals increase in mesenchymal markers and decrease in epithelial markers following inhibition of let-7d

Immunofluorescence confirmed the results at the protein level (Fig 21). A549 cells transfected with a let-7d inhibitor stained positive (red) for CDH2, VIM and ACTA2 48 h post-transfection, while mock-transfected cells did not express positive staining. The green fluorescence represents cytokeratin, an epithelial marker. The red fluorescence denotes the mesenchymal markers (CDH2, VIM and ACTA2). Nuclei were counterstained with DAPI. While red staining is observed in cells transfected with let-7d inhibitor (right panel), there is no staining in cells transfected with a control oligonucleotide (left panel).

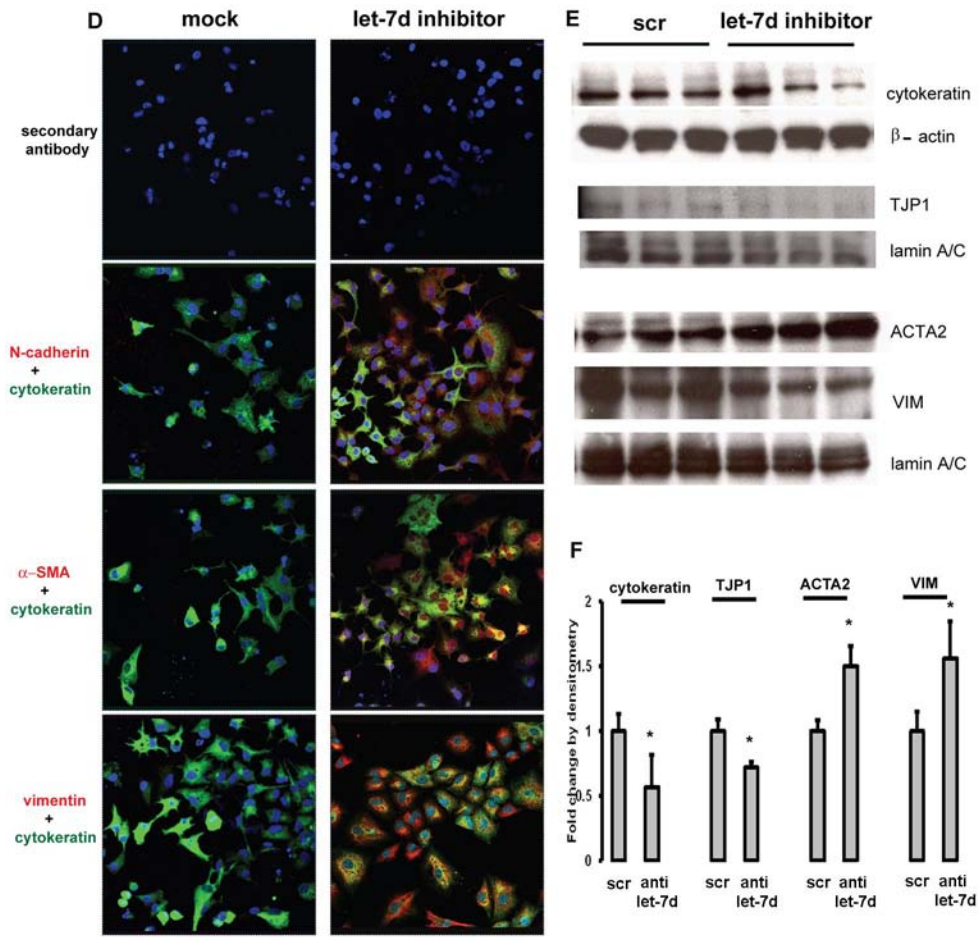


**Figure 21. Inhibition of let-7d demonstrates an increase in mesenchymal proteins in A549 cells.**

RLE-6TN cells transfected with a let-7d inhibitor for 72h show increase expression of mesenchymal markers ACTA2 and VIM and decrease in epithelial markers cytokeratin and TJP1 (Fig. 21) by immunoblotting suggestive of EMT.

### 3.6.3 Let-7d-induced EMT is not totally dependent on HMGA2

To determine if the EMT seen after inhibiting let-7d is due to the corresponding increase in HMGA2, we inhibited both let-7d and HMGA2 simultaneously. As seen in Fig. 22, the

mesenchymal markers increased after let-7d inhibition but though CDH2 returned to baseline after simultaneous inhibition of HMGA2, ACTA2 and VIM remained elevated.

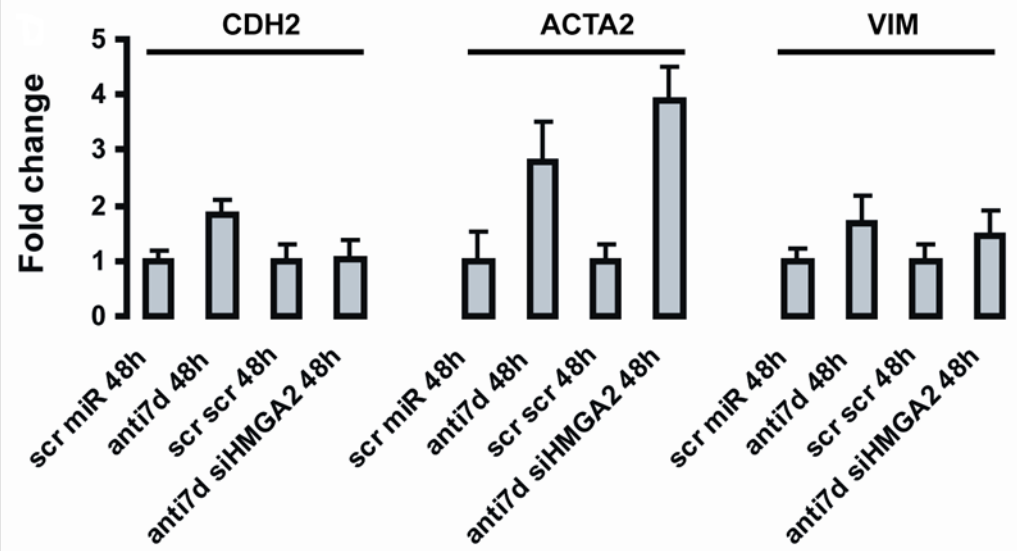


**Figure 22. EMT caused by reduced let-7d is not totally dependent on HMGA2.**

A possible explanation for this phenomenon could be that let-7d targets other fibrosis-relevant genes along with HMGA2. These genes maintain the mesenchymal phenotype irrespective of a change in HMGA2. A second possibility is that let-7d along with a few other microRNAs may be targeting HMGA2 together. For example, miR-17, miR92 and miR-26 are all predicted to target HMGA2. Also, we found that miR-30 inhibition increase HMGA2 which is discussed in the next section. Hence HMGA2 may be a direct target of miR-30 but this needs to be proven.

## 3.7 INHIBITION OF MIR-30 FAMILY

There are 5 members in the miR-30 family- miR-30a through miR-30e, all being downregulated in IPF. To perform functional studies, it would have been quite toxic to the cells to transfect them with five different inhibitors, one for each member. To overcome this problem we designed an inhibitor which could inhibit three members miR-30a, miR-30d and miR-30e that have similar sequences than the other two members. We adapted the design from Mott *et al*. [179]. We designed a locked nucleic acid (LNA)/DNA oligonucleotide. Based on sequence identity within the family, LNA bases were positioned at bases shared by all family members. Eight LNA residues were placed into two blocks of four. In the figure below, the LNA bases are marked in red.

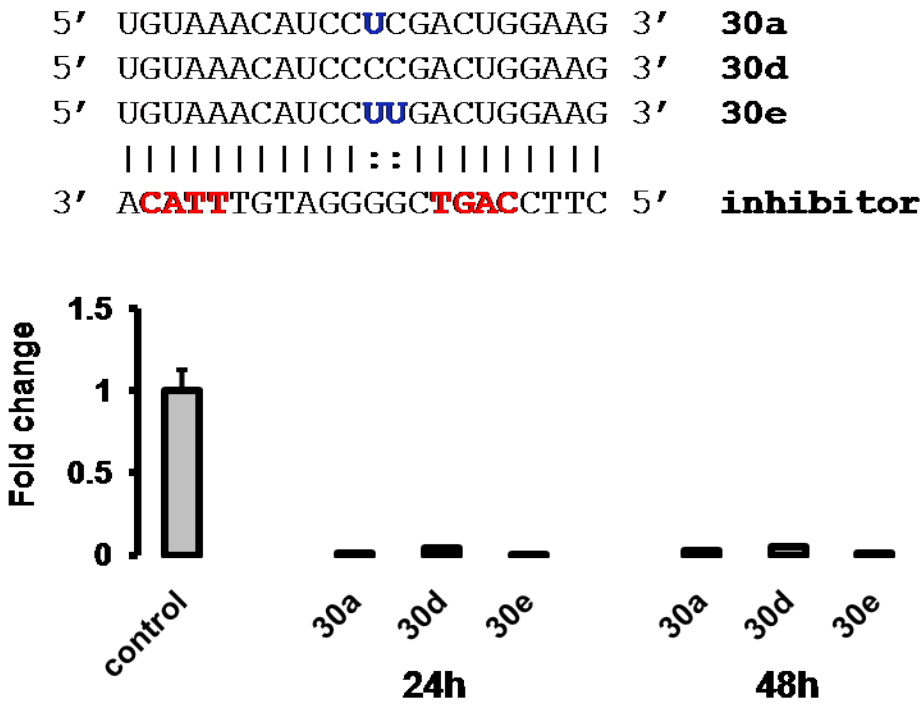


**Figure 23. Inhibition of miR-30 members by a single oligonucleotide.**

As seen in the figure above, transfection of 50nM of this oligonucleotide, totally knocked down the three members. RNA isolated 24h and 48h after transfection revealed an increase in HMGA2, VIM, EDNRA and ADAM19. All these genes are increased in IPF and/or EMT. Jain *et al*. showed that endothelin-1 induces alveolar EMT through endothelin type A receptor (EDNRA)-mediated production of TGF-β1 [54]. We chose to test expression of VIM, EDNRA and ADAM19 because they are predicted targets of the miR-30 family by TargetScan.

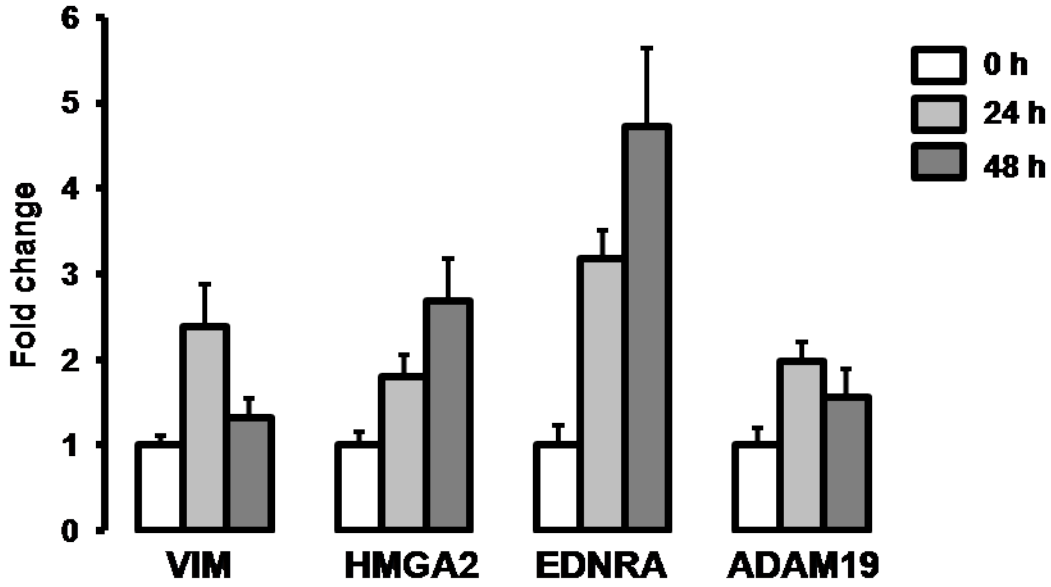


**Figure 24. Inhibition of miR-30 results in increase in genes upregulated in IPF.**

Two members of the miR-30 family, miR-30c and miR-30e are in the intron of nuclear transcription factor Y, gamma (*NFYC)*. NFYC represses Smad2 and Smad3 transactivating activity either by direct binding to the Smad-responsive element or through their association with the Smad-interacting transcription factor FAST-2 (forkhead activin signal transducer-2) [180].

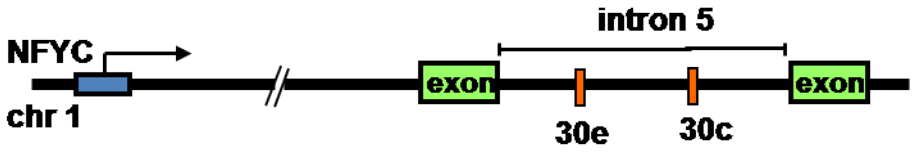


**Figure 25. miR-30c and miR-30e are in the intron of NFYC.**

Generally intronic microRNAs are transcribed with their host genes in which case, NFYC should also be downregulated in IPF. We did find NFYC to be decreased in IPF by microarrays and real-time PCR highly suggestive of cotranscription of NFYC, miR-30e and miR-30c but this needs to be proven by transcriptional gene silencing of NFYC.

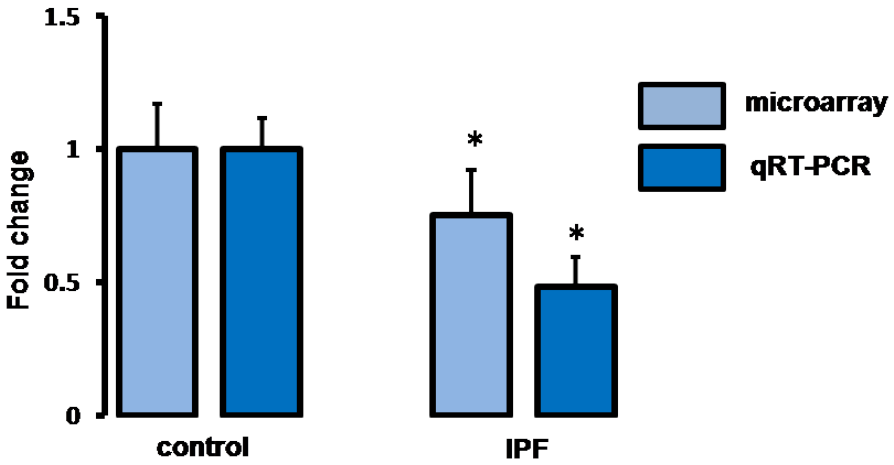


**Figure 26. NFYC is down-regulated in IPF.**

## 3.8 INHIBITION OF LET-7D *IN VIVO*

### 3.8.1 Dosage optimization

*In vitro* inhibition of let-7d led to EMT in A549 and RLE-6TN cell lines and NHBE primary cells. To determine the effects of let-7d inhibition *in-vivo* we administered the let-7d antagomir designed as previously described [173]. Initially we administered the antagomir at a dose of 80 mg/kg body weight to mice. This dose was very toxic which caused death of two of the four mice. The two remaining mice were very sick and were sacrificed after a single dose. Their lungs were grossly hemorrhagic. This single dose was enough to knock down let-7d totally. We reduced the dose to 10 mg/kg body weight and administered it intratracheally into the lungs of 4 mice on three consecutive days and sacrificed the mice on the fourth day. At this dose too the mice appeared sick and the lungs were hemorrhagic and it was impossible to maintain them longer. To better observe the long term effects of let-7d inhibition we reduced the dose to 5 mg/kg body weight and treated the animals for 17 days. The antagomir was given on days 1, 2, 3, 8, 9, 10, 15, 16 and 17. At this dose we detected a significant decrease in let-7d in the lung (Fig. 27) but the mice did not demonstrate any discomfort. Control mice were administered an equal volume of saline.

### 3.8.2 Knockdown of let-7d

The intratracheal administration of the let-7d antagomir caused a complete knockdown of let-7d in the lung with all the three doses *viz.* 80, 10 and 5 mg/kg (Fig. 27).

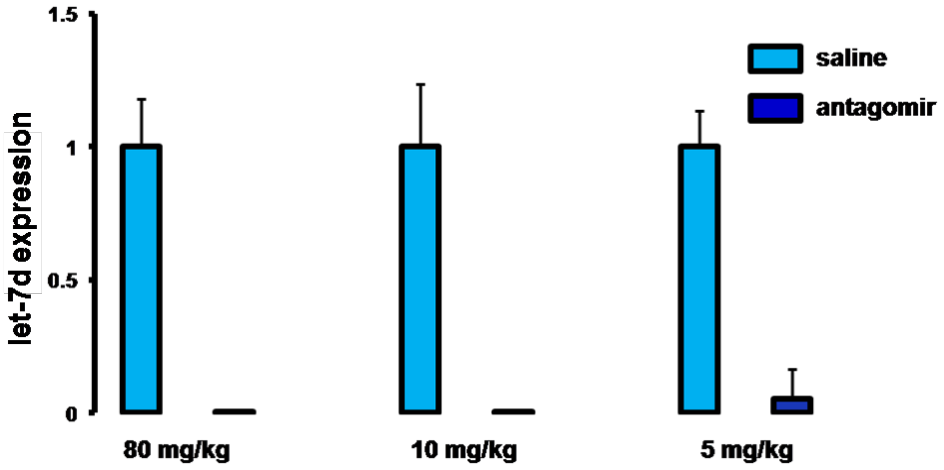


**Figure 27. Knockdown of let-7d by the antagomir at different doses.**

After we optimized the dose to 5 mg/kg body weight, we designed a scrambled oligonucleotide control. This scrambled control had four mismatches in the sequence but was identical to the antagomir in terms of the base modifications. Let-7d was knocked down significantly using the antagomir in comparison to the scrambled oligonucleotide.

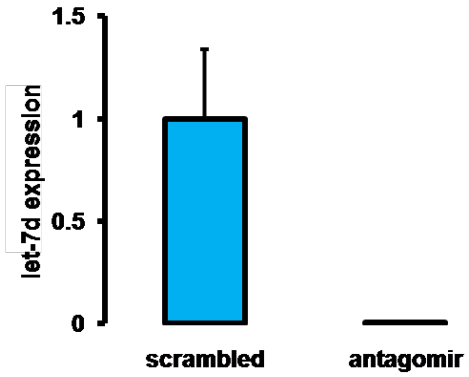


**Figure 28. Knockdown of let-7d by the antagomir in comparison to the scrambled control.**

### 3.8.3 Profibrotic changes after let-7d inhibition *in vivo*

#### 3.8.3.1 In comparison to saline control

We assessed the degree to which we were able to induce EMT in the mice lungs after administering 10 mg/kg antagomir for 3 days. Let-7d inhibition caused a significant decrease in the expression of the epithelial markers CDH1 and ZO-1 and a significant increase in COL1A1 and HMGA2 expression in the lung (Fig. 29).

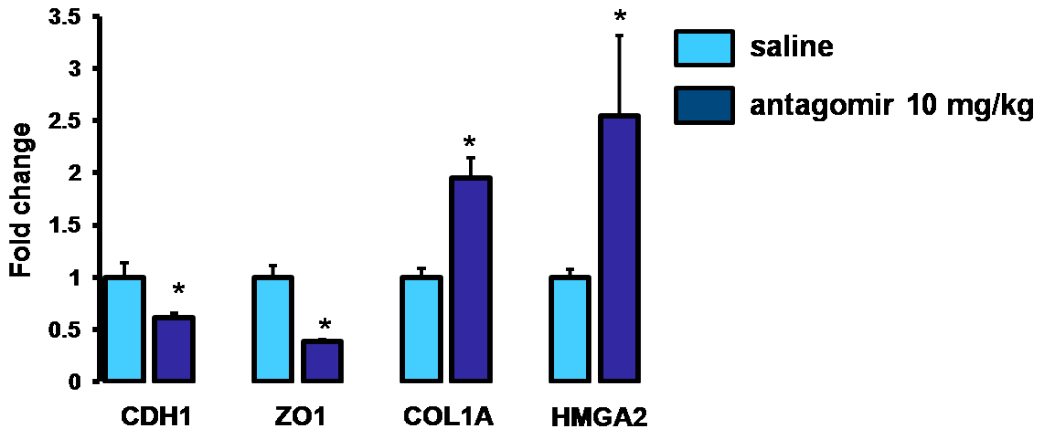


**Figure 29. Reduced epithelial markers and increased mesenchymal markers following antagomir administration.**

In the extended protocol, in which the mice were treated for 17 days, we observed an increase in collagen and ACTA2 by Masson's trichrome and immunohistochemistry respectively. Masson's trichrome stain of formalin fixed mouse lung demonstrated increased thickening of alveolar septa and increased blue stain (red arrows) indicative of the presence of collagen in let-7d antagomir-treated lungs (Fig. 30A). Panels (i), (iii) are saline lungs and panels (ii), (iv) are antagomir-treated lungs. The scale bars in (i) and (iii) denote 100 µm and those in (ii) and (iv) denote 25 µm. Quantitation of the blue stain revealed a 2.6 fold increase in

antagomir-treated lungs (Fig. 30C). Morphometric analysis showed that in the antagomir-treated lungs, the total tissue per field was increased by 21% relative to the control sections (Fig. 30B). For these quantitations, we selected images without airways and blood vessels to avoid any bias.

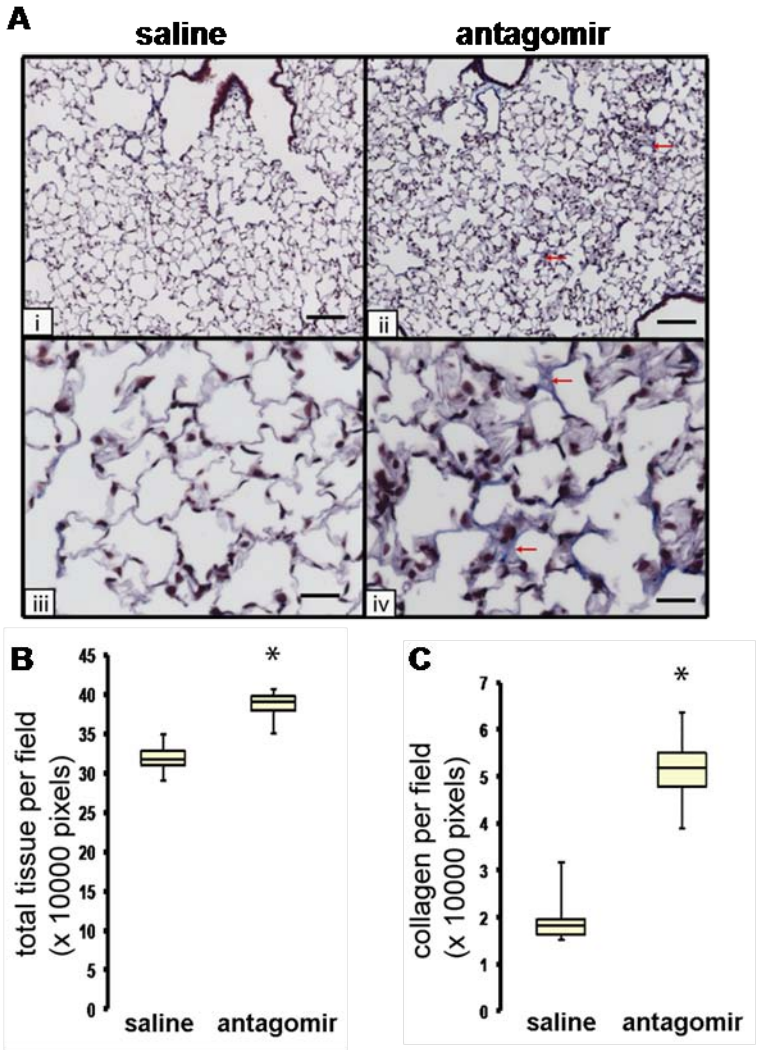


**Figure 30. Masson trichrome staining after 18 days of saline or antagomir treatment.**

Immunohistochemical staining for ACTA2 revealed enhanced immunoreactive protein (brown) in alveolar walls in antagomir-treated mice lungs that was not observed in saline treated mice (Fig. 31). Panels (i), (iii) are saline lungs and panels (ii), (iv) are antagomir-treated lungs. The scale bars in (i) and (iii) denote 100 µm and those in (ii) and (iv) denote 25 µm. Manual

counting of the ACTA2-positive cells revealed a significant increase in the antagomir-treated lungs.

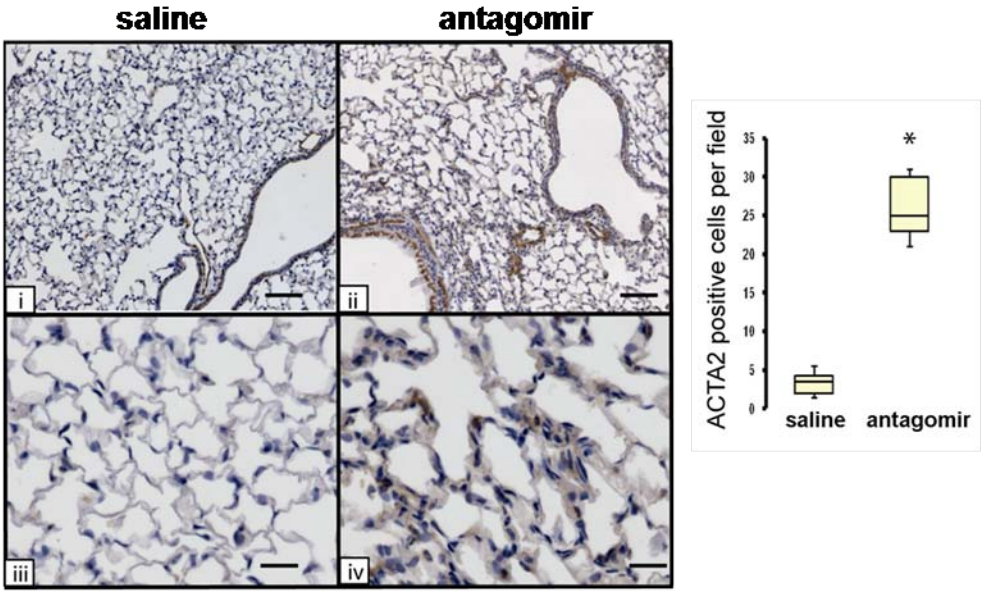


**Figure 31. Immunolocalization of α-smooth muscle actin after 18 days of saline or antagomir treatment.**

### 3.8.3.2 In comparison to the scrambled oligonucleotide

We repeated the same extended protocol of treating the mice for 17 days but used the scrambled oligonucleotide this time to control for any changes caused by introduction of the oligonucleotide itself. We observed and increase in collagen, ACTA2 and CDH2 in the antagomir-treated lungs but VIM and fibroblast specific protein 1 (FSP1) were unchanged by real-time PCR.

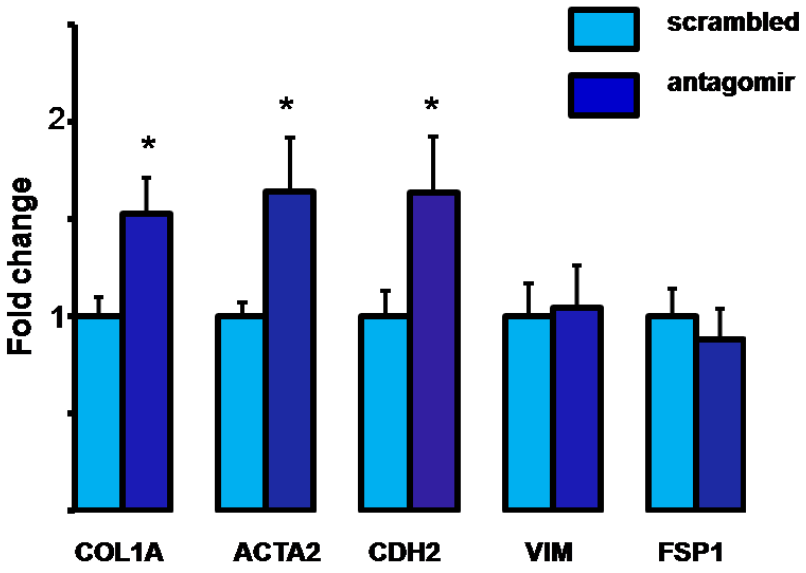


**Figure 32. Increase in mesenchymal markers following antagomir administration.**

Since RAS is a known direct target of let-7 family of microRNAs, we used KRAS as a positive control. Immunohistochemistry for KRAS showed increased staining for KRAS in alveolar epithelial cells and macrophages as demonstrated by the positive brown stain (Fig. 33).

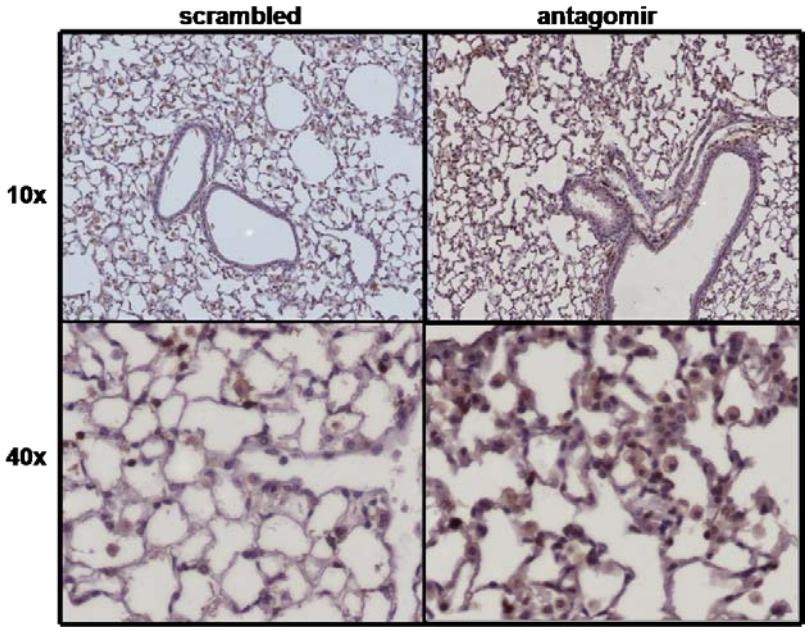


**Figure 33. Increase in RAS in antagomir lungs.**

Masson trichrome staining for collagen shows increased blue staining for collagen in antagomir lungs and thickening of alveolar septae (Fig. 34).

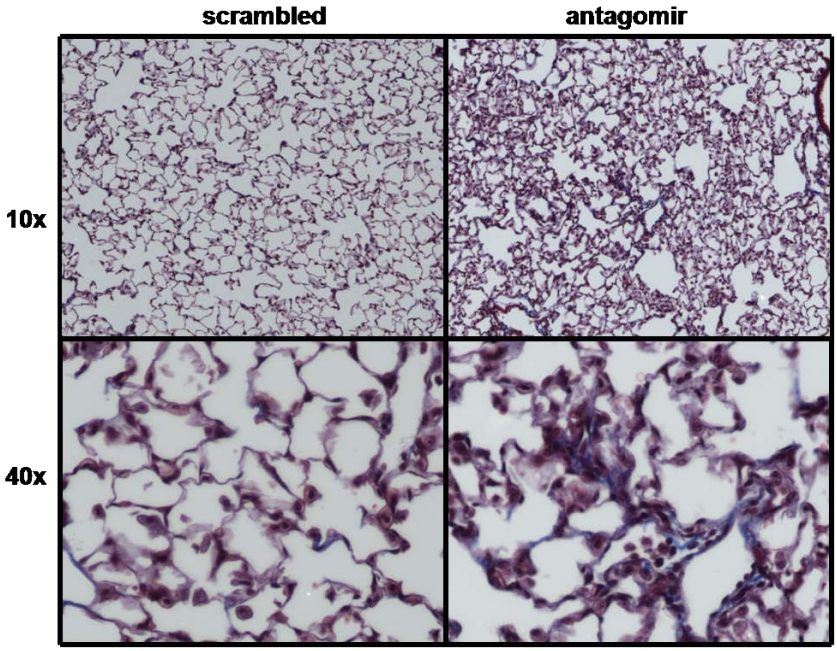


**Figure 34. Increase in collagen in antagomir lungs.**

Immuhistochemical staining for ACTA2 and CDH2 both show increased brown staining in antagomir treated lungs but these changes were more focal and seen in certain areas of the lung sections (Fig. 35, 36).

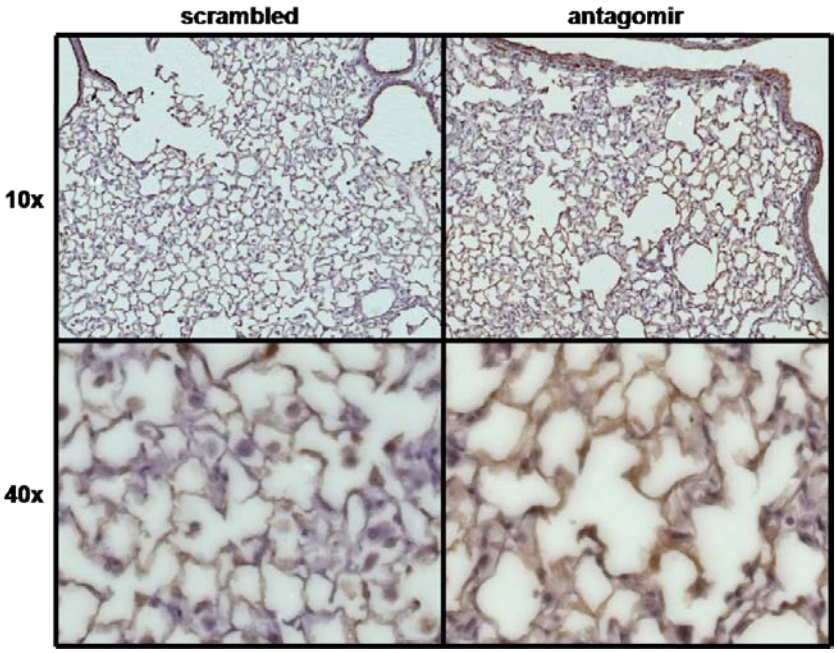


**Figure 35. Increase in ACTA2 in antagomir lungs.**

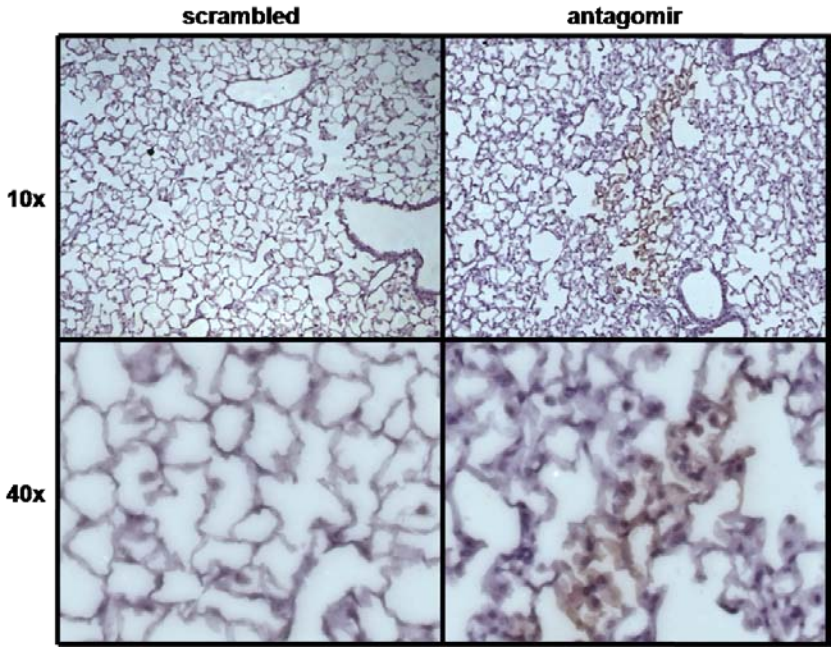


**Figure 36. Increase in CDH2 in antagomir lungs.**

To demonstrate EMT in the antagomir treated lungs, we colocalized an alveolar epithelial marker, surfactant protein C (SPC) with the mesenchymal markers, FSP1 and ACTA2 by

immunofluorescence (Fig. 37). During the process of EMT, the alveolar epithelial cells gradually lose the epithelial markers and gain mesenchymal markers but during a brief period express both. The white arrows point to cells expressing both markers. The red arrows point to cells expressing only SPC indicating that there are some cells which have still not undergone EMT.

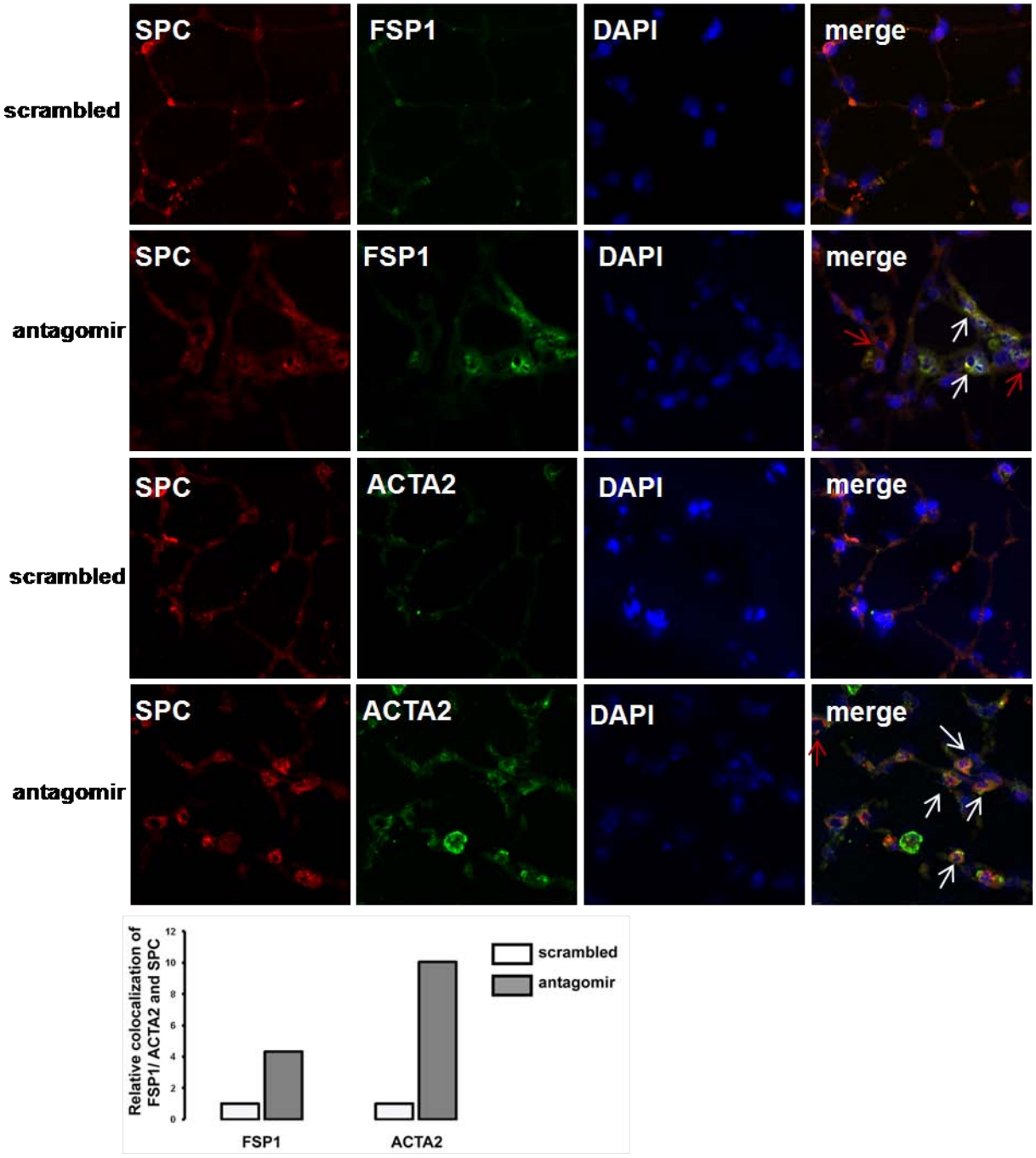


**Figure 37. Colocalization of FSP1 and ACTA2 with SPC in antagomir lungs.**

Fig. 37 shows the relative average colocalization of epithelial and mesenchymal markers in five different fields of each slide. For the specific images shown in the figure, there was 38% and 41% colocalization of the total tissue for FSP1 and ACTA2 respectively. The scrambled control sections however showed only about 6% colocalized area per section.

Taken together these results suggest that *in-vivo* inhibition of let-7d in the lung causes changes consistent with changes in epithelial cell phenotype (decrease in CDH1 and ZO1) and consistent with early fibrosis (thickened alveolar septa, increased collagen, ACTA2 and CDH2).

# 4.0 DISCUSSION

In this study we explored the expression, regulation and potential role of microRNAs in IPF. Among the downregulated microRNAs in IPF lungs we focused on let-7d and discovered that it was directly transcriptionally inhibited by the key pro-fibrotic cytokine TGF-β. *In-vitro* inhibition of let-7d induced an increase in mesenchymal markers and a corresponding decrease in epithelial markers in lung epithelial cell lines suggestive of EMT. *In-vivo* inhibition of let-7d in mouse lungs caused alveolar septal thickening, decreased expression of epithelial markers and increase in collagen, ACTA2 and CDH2 consistent with early fibrotic changes. We demonstrated EMT by colocalizing FSP1 and ACTA2 with the epithelial marker SPC. In IPF lungs let-7d expression was drastically diminished, while HMGA2 expression was increased in alveolar epithelial cells. Increased expression of HMGA2 was induced by let-7d inhibition *in-vitro* and TGF-β induced expression of HMGA2 was inhibited by let-7d expression suggesting that the concomitant decrease in let-7d and increase in HMGA2 in human lungs were associated. Taken together our findings suggest that let-7d inhibition is a key regulatory event in the dramatic phenotypic changes that happen in the alveolar epithelium in IPF.

In this study we demonstrate the influence of TGF-β, the key profibrotic cytokine and a regulator of EMT [181] on the expression of a microRNA through direct effect on its promoter. This result is consistent with the recent genome scale analysis of microRNA promoters and evidence for binding by stem cell transcription factors as well as RNA polymerase II that suggest

that the expression of many microRNAs is under dynamic transcriptional regulation by transcription factors [182, 183]. So far changes in let-7 microRNAs expression levels have been mostly attributed to their localization to fragile sites [184] to post-transcriptional modification [185] or to epigenetic changes [143]. Our discovery that let-7d is directly inhibited by TGF-β adds a new potential mechanism for regulation of microRNAs and may have important therapeutic implication as inhibitors of TGF-β signaling and activation are currently evaluated for cancer and fibrosis. Furthermore, the suggestion that some of TGF-β effects on epithelial cells may be mediated through microRNAs may have significant implications in better understanding the profound and sustained effects of TGF-β on cell and organ phenotype.

## 4.1 LET-7 FAMILY ALSO TARGETS OTHER FIBROSIS RELEVANT GENES

The let-7 family of microRNAs was one of the first discovered [136] and the most extensively studied; however this is the first time a member of the let-7 family has been implicated in a non-tumor disease. Members of the let-7 family are temporally regulated microRNAs which coordinate developmental timing [136]. They are considered tumor suppressors, regulating RAS and many cell cycle genes [186] and their expression is supposed to sustain an “epithelial” gene signature [187]. Among the genes suppressed by the let-7 family is HMGA2, a structural transcriptional regulator expressed in early embryonic development, some benign tumors and lung cancer [176]. In the context of IPF it is of interest to note that HMGA2 confers a growth advantage to fibroblasts as evident by the retarded growth in *hmga2*-deficient mouse embryonic fibroblasts compared to wild-type fibroblasts [188] and is also a mediator of TGF-β induced EMT [112]. However, while we found a dramatic decrease in let-7d expression

accompanied by an increased in HMGA2 in human IPF lungs, and demonstrated that inhibition of let-7d leads to EMT *in-vitro* and to early fibrotic changes *in-vivo*, we do not have direct evidence that this effect is solely mediated through HMGA2. As seen in Fig. 22, the mesenchymal markers increased after let-7d inhibition but though CDH2 returned to baseline after simultaneous inhibition of HMGA2, ACTA2 and VIM remained elevated.

A more realistic interpretation at this stage would be that in the lung, downregulation of let-7d leads to upregulation of HMGA2 as well as other fibrosis relevant targets of let-7 such as RAS, IGF1, IGF1R (Fig. 38) [178] and thus leads to the profound and sustained changes in cellular phenotype that are indeed observed in IPF.

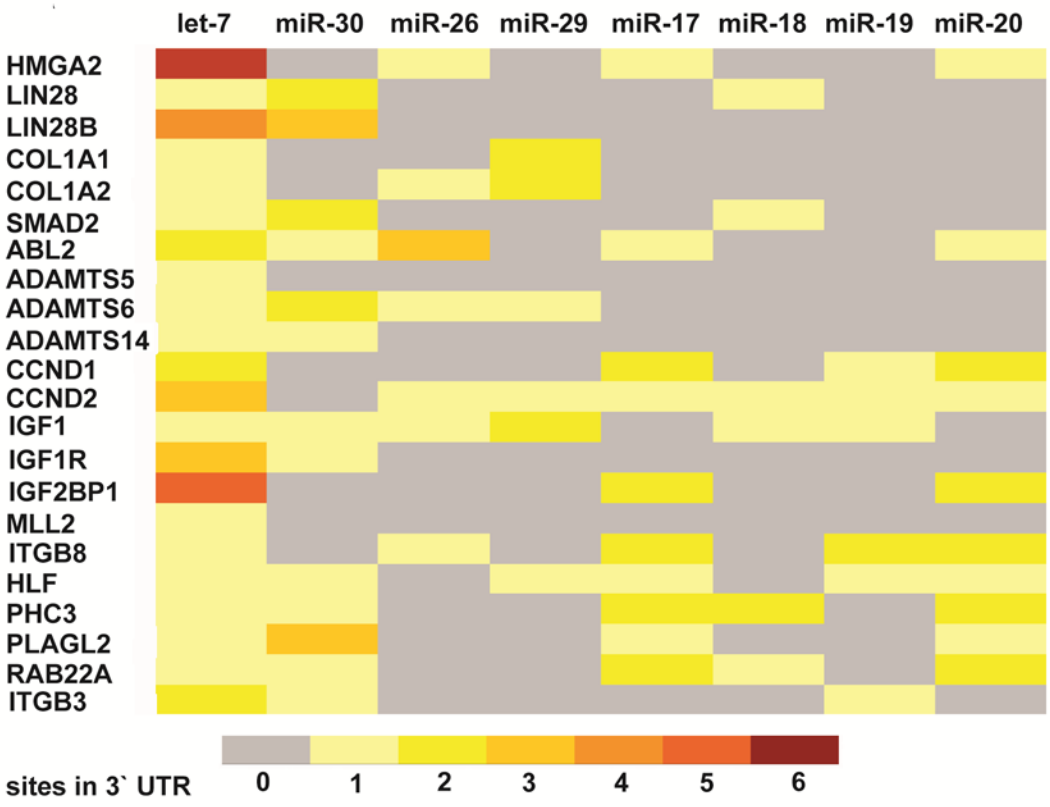


**Figure 38. Overlapping targets of microRNAs down-regulated in IPF.**

Fig. 38 depicts the computationally predicted targets of the microRNAs down regulated in our IPF dataset. These fibrosis-relevant and EMT-relevant targets and the predicted sites of each miRNA in their 3' UTRs were chosen from TargetScan database. The fact that let-7 inhibition is sufficient to induce changes consistent with EMT *in-vitro* and expression of mesenchymal markers as well as thickening of alveolar septum indicative of early fibrosis *in-vivo* also suggests an effect mediated through modification of the expression of multiple fibrosis relevant genes and not just a single gene.

It is important to note that while we focus on let-7d, the downstream effects of let-7d overexpression or inhibition are probably common to all members of the let-7 family of microRNAs.

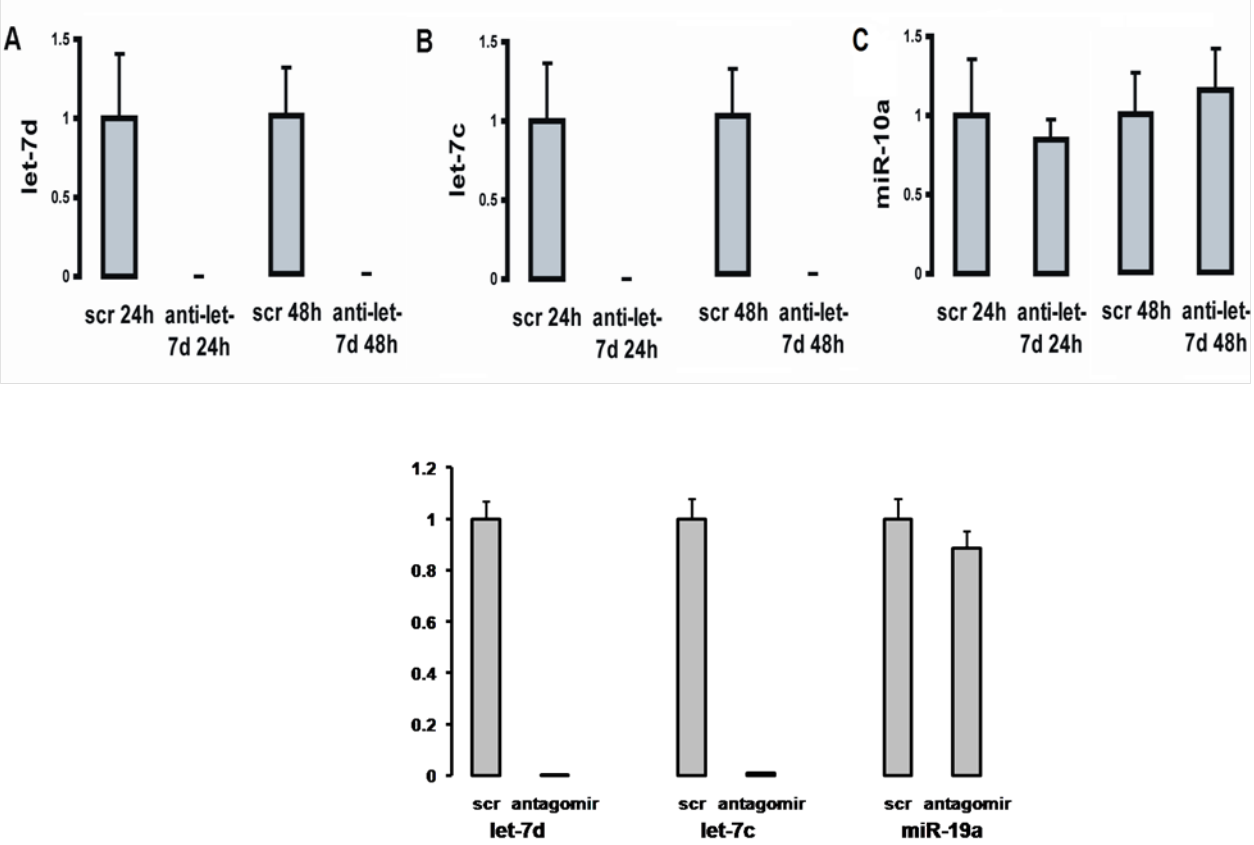


**Figure 39. Specificity of the let-7 inhibitor used *in vitro* and *in vivo*.**

While the inhibitory effects we describe do not go through microRNAs that are not members of the let-7 family it is highly unlikely that this effect will be mediated only through let-7d and not through other members of the family. As seen in the figure above, the let-7d inhibitor used *in vitro* (upper panel) or the antagomir used *in vivo* (lower panel) also inhibited a member of the same family, let-7c, but not miR-10a or miR-19a, two randomly selected microRNAs.

## 4.2 ROLE OF OTHER MICRORNAS

Our results add to previous results that implicated a role for inhibition of microRNAs in EMT [120-123]. The miR-200 family prevents EMT by targeting the transcription factors ZEB1 and SIP1 that repress E-cadherin, an epithelial cell marker [120-123]. Similar to let-7d, TGF-β stimulation also decreased expression of the miR-200 family. Overexpression of the miR-200 family could not completely block EMT [121] suggesting that let-7d and miR-200 family may be acting synergistically possibly with a few other microRNAs in preventing EMT. While the current study does not directly overlap the putative pathway of miR-200 family, there is no doubt that there may be multiple signaling cascades likely to be at work in a complex cellular transition such as EMT.

Inhibition of miR-30 family members led to an increase in VIM, ADAM19, HMGA2 and EDNRA. They may be direct targets of miR-30 which needs to be proven by 3` UTR reporter assays. Of particular interest are EDNRA and connective tissue growth factor (CTGF). It has been shown that endothelin-1 is an important mediator of EMT in alveolar epithelial cells, acting through EDNRA–mediated TGF-β production [54]. Connective tissue growth factor (CTGF) is a known target of miR-30 [189]. CTGF is a growth and chemotactic factor for fibroblasts encoded

by an immediate early gene that is transcriptionally activated by TGF-β [190]. It is induced by a number of profibrotic mediators and localizes to proliferating type II alveolar epithelial cells and activated fibroblasts [191]. CTGF is a proven target of miR-30 and has an important role in the control of structural changes in the extracellular matrix of the myocardium [189].

On the basis of studies on endothelin, miR-200 and from our data, it is highly likely that let-7d, miR-30 and miR-200 act synergistically to maintain the epithelial cell phenotype.

## 4.3 MICRORNA EXPRESSIONS SIMILAR TO THOSE IN IPF

Microarray analysis identified an IPF specific gene expression signature characterized by the up-regulation of genes indicative of active tissue remodeling, including extracellular matrix and a large number of myofibroblast/smooth muscle cell–associated and epithelial cell–related genes [6, 8, 11, 13]. IPF lungs are also enriched with genes associated with lung development, indicating that embryonic signaling pathways involved in epithelial cell plasticity may be aberrantly activated [8, 11, 13, 66]. It is possible that as genes in different organs or during different embryonic stages maintain the epithelial cell phenotype, microRNAs have a similar role. We found that most of the microRNAs downregulated in IPF were also downregulated in fetal lung tissues as assessed by real-time PCR (Fig. 6).

The microRNA profiling of rat lungs exposed to cigarette smoke for 28 days revealed a decrease in the let-7 family, miR-26 and miR-30 families [192]. These microRNAs are also decreased in IPF which has smoking as one of the risk factors for the disease. Schembri *et al*. studied the bronchial airway microRNA expression of smokers and non-smokers. Members of the miR-17 ~ 92 cluster and miR-30a were downregulated in smokers [193]. The let-7 family,

miR-30, miR-26 families are downregulated in many cancers [194-201] .This suggests that the microRNA signature of EMT is similar irrespective of the pathological or physiological condition being studied such as development, environmental factors like smoking or diseases like IPF and cancer.

## 4.4 PROPOSED MODEL

On the basis of our data and what is published in literature, we propose a model for EMT in IPF (Fig. 40). After the initial and persistent injury to the alveolar epithelial cell, there is an influx of cytokines like TGF-β, ET−1 and CTGF. One of the reasons for the increase in ET-1 and CTGF could be the reduction in miR-30. TGF-β synthesis is increased by ET-1 and vice versa. Increase in TGF-β phosphorylates the SMADs. SMAD3 transcriptionally inhibits let-7d which in turn negatively regulates HMGA2, RAS and possibly IGF1 and IGF1R. NFYC tries to maintain homeostasis by binding to the SMAD responsive element and suppresses SMAD3 activity. SMAD4 increases transcription of HMGA2 whereas SMAD3 and HMGA2 co-operatively increase SNAI1 transcription. TGF-β inhibits the ID molecules which in turn prevent down-regulation of CDH1 by preventing the E2A transcription factors from binding to the CDH1 promoter. The targets of let-7 viz. HMGA2, RAS, IGF, IGF1R increase the transcription factors SNAI1, SNAI2, TWIST and ZEB1. These inhibit CDH1 and other targets ultimately leading to EMT.

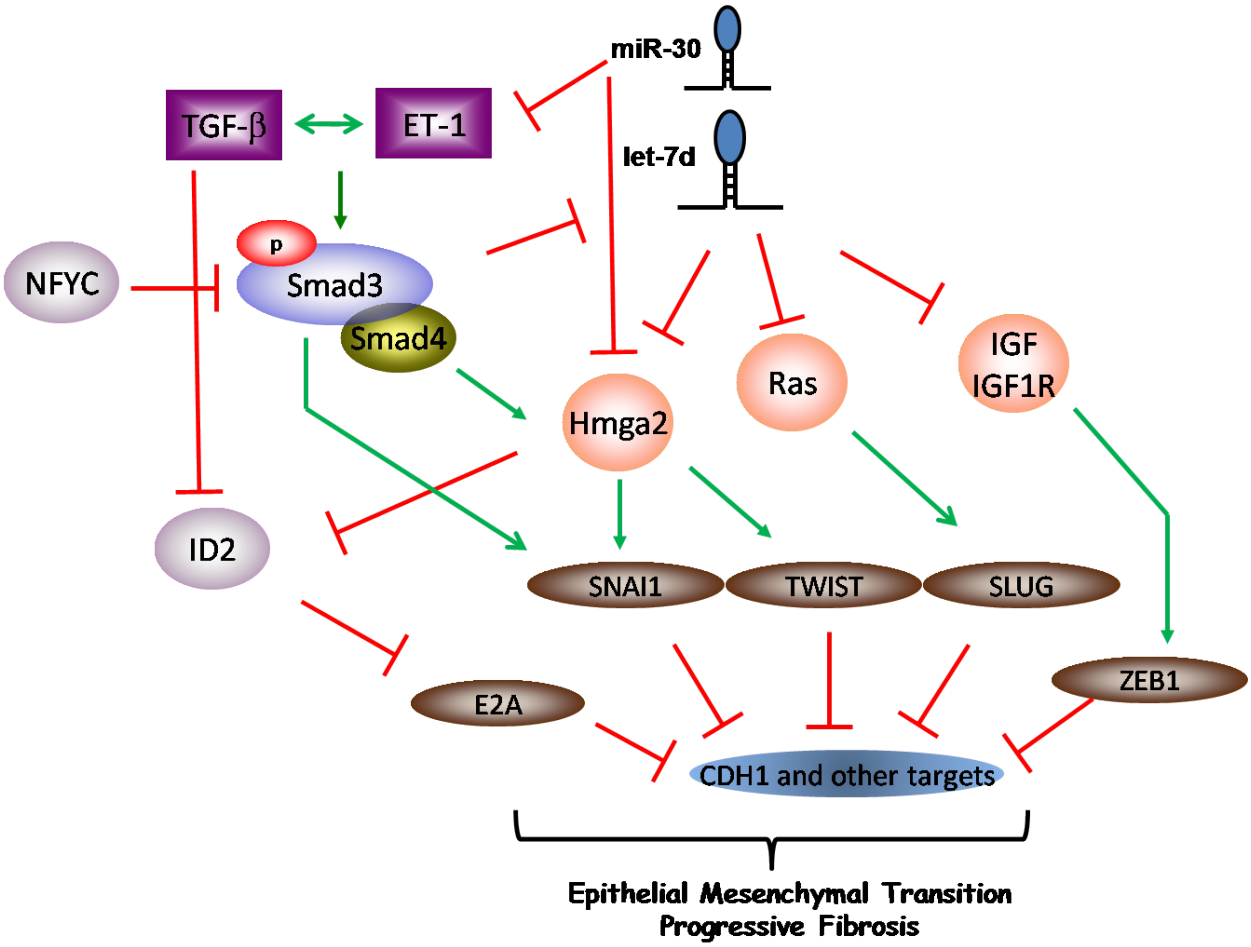


**Figure 40. Model for EMT in IPF.**

# 5.0 CONCLUDING REMARKS

## 5.1 SUMMARY

In summary, we demonstrate that IPF lungs are different from control lungs in their microRNA repertoire. We discovered that let-7d, a microRNA significantly downregulated in IPF, is negatively transcriptionally regulated by TGF-β. Furthermore, inhibition of let-7d alone is sufficient to cause EMT changes in A549, RLE-6TN cells and NHBE cells. Concomitant with let-7d down-regulation in IPF lungs, we found significant increases in lung expression of HMGA2 suggesting that let-7 inhibition of HMGA2 is released in IPF lungs. Finally, we demonstrate that let-7 inhibition *in-vivo* in the lung may cause changes in the lung alveolar epithelium with increases in mesenchymal markers, decreases in epithelial markers and thickening of alveolar septa. The discovery of the downregulation of let-7d in IPF, its regulation by TGF-β and its potential role in EMT and fibrosis may have important implications in our understanding of the molecular mechanisms underlying IPF as well lead to the development of new therapeutic interventions in this devastating and incurable disease.

## 5.2 FUTURE DIRECTIONS

Elucidation of the mechanism and pathway through which let-7d exerts its action in inducing EMT is essential. Additionally, this study is not complete until a therapeutic role for let-7 is established.

Inhibition of HMGA2 was not enough to stop EMT which suggests that let-7d may be exerting its effects by acting on a number of IPF-relevant targets which include RAS, IGF1, IGF1R and possibly a few others. The possibility that let-7d could be targeting these other genes needs to be explored. A few microRNAs decreased in IPF have common targets. For example, HMGA2 is a computationally predicted target of miR-17, miR-26 and miR-92 and could possibly be a direct target of miR-30 which needs to be proven by a reporter assay. Repeating the *in vitro* experiments with inhibition of all or a combination of these microRNAs will be beneficial.

Finally, a few *in vivo* experiments in mice are warranted. First, using transgenic mice like HMGA2 or RAS knockouts will help to dissect the pathway through which reduction in let-7d causes EMT. Secondly, administration of the let-7d antagomir intravenously will reinforce the fact that let-7d reduction leads to EMT in other organs as well such as the kidney in which EMT is well-studied. Lastly, resolution of fibrosis by administration of a let-7d mimic to mice having bleomycin-induced lung fibrosis will establish a therapeutic role for let-7d.

# APPENDIX A

## LIST OF ANTIBODIES

**Table 2. List of antibodies used for immunoblotting and their relative concentrations.**

| Antibody | Type | Company | Concentration |
|---|---|---|---|
| ACTA2 | rabbit monoclonal | Abcam | 1:20000 |
| VIM | mouse monoclonal | Abcam | 1:100 |
| cytokeratin | rabbit polyclonal | Abcam | 1:1000 |
| actin | mouse monoclonal | Sigma | 1:4000 |
| laminin A/C | rabbit polyclonal | Santa Cruz | 1:1000 |
| TJP1 | rabbit polyclonal | Santa Cruz | 1:500 |

**Table 3. List of antibodies used for immunofluorescence and their relative concentrations.**

| Antibody | Type | Company | Concentration |
|---|---|---|---|
| CDH2 | rabbit polyclonal | Abcam | 1:500 |
| VIM | mouse monoclonal | Abcam | 1:1000 |
| ACTA2 | rabbit monoclonal | Abcam | 1:600 |
| cytokeratin | mouse monoclonal | Abcam | 1:500 |

Table 3 contd.

| | | | |
|---|---|---|---|
| SPC | rabbit polyclonal | Abcam | 1:600 |
| FSP1 | rabbit polyclonal | Abcam | 1:600 |
| HMGA2 | rabbit polyclonal | Abcam | 1:50 |

# APPENDIX B

## ISH DATA WITH FVC

**Table 4. let-7d counts of in situ hybridization and corresponding forced vital capacities.**

| case | Diagnosis | let-7d positive AECs/mm$^2$ | FVC (% pred) |
|---|---|---|---|
| 1 | IPF | 16 | 59 |
| 2 | IPF | 16 | 60 |
| 3 | IPF | 10 | 51 |
| 4 | IPF | 10 | 48 |
| 5 | IPF | 16 | 58 |
| 6 | IPF | 26 | 60 |
| 7 | IPF | 25 | 59 |
| 8 | IPF | 20 | 65 |
| 9 | IPF | 15 | 50 |
| 10 | IPF | 20 | 55 |
| 11 | IPF | 5 | 51 |
| 12 | IPF | 2 | 48 |
| 13 | IPF | 20 | 55 |
| 14 | IPF | 40 | 81 |
| 15 | IPF | 30 | 66 |
| 16 | IPF | 28 | 62 |
| 17 | IPF | 17 | 60 |
| 18 | IPF | 21 | 56 |
| 19 | IPF | 33 | 70 |
| 20 | IPF | 31 | 65 |
| 21 | IPF | 19 | 63 |
| 22 | IPF | 14 | 59 |
| 23 | IPF | 13 | 54 |

Table 4 contd.

| | | | |
|---|---|---|---|
| 24 | IPF | 15 | 50 |
| 25 | IPF | 8 | 53 |
| 26 | IPF | 7 | 55 |
| 27 | IPF | 20 | 56 |
| 28 | IPF | 18 | 48 |
| 29 | IPF | 12 | 43 |
| 30 | IPF | 27 | 61 |
| 31 | IPF | 10 | 67 |
| 32 | IPF | 9 | 49 |
| 33 | IPF | 17 | 48 |
| 34 | IPF | 15 | 56 |
| 35 | IPF | 14 | 67 |
| 36 | IPF | 18 | 52 |
| 37 | IPF | 22 | 54 |
| 38 | IPF | 15 | 49 |
| 39 | IPF | 16 | |
| 40 | IPF | 25 | |
| 41 | Control | 55 | |
| 42 | Control | 58 | |
| 43 | Control | 48 | |
| 44 | Control | 65 | |
| 45 | Control | 77 | |
| 46 | Control | 55 | |
| 47 | Control | 65 | |
| 48 | Control | 47 | |
| 49 | Control | 61 | |
| 50 | Control | 59 | |
| 51 | Control | 65 | |
| 52 | Control | 58 | |
| 53 | Control | 82 | |
| 54 | Control | 44 | |
| 55 | Control | 46 | |
| 56 | Control | 24 | |
| 57 | Control | 28 | |
| 58 | Control | 84 | |
| 59 | Control | 80 | |
| 60 | Control | 75 | |

## BIBLIOGRAPHY


1. Selman, M., T.E. King, and A. Pardo, *Idiopathic pulmonary fibrosis: prevailing and evolving hypotheses about its pathogenesis and implications for therapy.* Ann Intern Med, 2001. **134**(2): p. 136-51.

2. Raghu, G., et al., *Incidence and prevalence of idiopathic pulmonary fibrosis.* Am J Respir Crit Care Med, 2006. **174**(7): p. 810-6.

3. *American Thoracic Society. Idiopathic pulmonary fibrosis: diagnosis and treatment. International consensus statement. American Thoracic Society (ATS), and the European Respiratory Society (ERS).* Am J Respir Crit Care Med, 2000. **161**(2 Pt 1): p. 646-64.

4. *American Thoracic Society/European Respiratory Society International Multidisciplinary Consensus Classification of the Idiopathic Interstitial Pneumonias. This joint statement of the American Thoracic Society (ATS), and the European Respiratory Society (ERS) was adopted by the ATS board of directors, June 2001 and by the ERS Executive Committee, June 2001.* Am J Respir Crit Care Med, 2002. **165**(2): p. 277-304.

5. Cosgrove, G.P., et al., *Pigment epithelium-derived factor in idiopathic pulmonary fibrosis: a role in aberrant angiogenesis.* Am J Respir Crit Care Med, 2004. **170**(3): p. 242-51.

6. Pardo, A., et al., *Up-regulation and profibrotic role of osteopontin in human idiopathic pulmonary fibrosis.* PLoS Med, 2005. **2**(9): p. e251.

7. Rosas, I.O., et al., *MMP1 and MMP7 as potential peripheral blood biomarkers in idiopathic pulmonary fibrosis.* PLoS Med, 2008. **5**(4): p. e93.

8. Selman, M., et al., *Gene expression profiles distinguish idiopathic pulmonary fibrosis from hypersensitivity pneumonitis.* Am J Respir Crit Care Med, 2006. **173**(2): p. 188-98.

9. Selman, M., et al., *Accelerated variant of idiopathic pulmonary fibrosis: clinical behavior and gene expression pattern.* PLoS One, 2007. **2**(5): p. e482.

10. Kaminski, N., et al., *Global analysis of gene expression in pulmonary fibrosis reveals distinct programs regulating lung inflammation and fibrosis.* Proc Natl Acad Sci U S A, 2000. **97**(4): p. 1778-83.

11. Zuo, F., et al., *Gene expression analysis reveals matrilysin as a key regulator of pulmonary fibrosis in mice and humans.* Proc Natl Acad Sci U S A, 2002. **99**(9): p. 6292-7.

12. Yang, I.V., et al., *Gene expression profiling of familial and sporadic interstitial pneumonia.* Am J Respir Crit Care Med, 2007. **175**(1): p. 45-54.

13. Konishi, K., et al., *Gene expression profiles of acute exacerbations of idiopathic pulmonary fibrosis.* Am J Respir Crit Care Med, 2009. **180**(2): p. 167-75.

14. Sebti, S.M., et al., *Bleomycin hydrolase: molecular cloning, sequencing, and biochemical studies reveal membership in the cysteine proteinase family.* Biochemistry, 1989. **28**(16): p. 6544-8.

15. Chaudhary, N.I., A. Schnapp, and J.E. Park, *Pharmacologic differentiation of inflammation and fibrosis in the rat bleomycin model.* Am J Respir Crit Care Med, 2006. **173**(7): p. 769-76.

16. Usuki, J. and Y. Fukuda, *Evolution of three patterns of intra-alveolar fibrosis produced by bleomycin in rats.* Pathol Int, 1995. **45**(8): p. 552-64.

17. Izbicki, G., et al., *Time course of bleomycin-induced lung fibrosis.* Int J Exp Pathol, 2002. **83**(3): p. 111-9.

18. Marshall, R.P., et al., *Adult familial cryptogenic fibrosing alveolitis in the United Kingdom.* Thorax, 2000. **55**(2): p. 143-6.

19. Hodgson, U., T. Laitinen, and P. Tukiainen, *Nationwide prevalence of sporadic and familial idiopathic pulmonary fibrosis: evidence of founder effect among multiplex families in Finland.* Thorax, 2002. **57**(4): p. 338-42.

20. Auwerx, J., et al., *Defective host defence mechanisms in a family with hypocalciuric hypercalcaemia and coexisting interstitial lung disease.* Clin Exp Immunol, 1985. **62**(1): p. 57-64.

21. DePinho, R.A. and K.L. Kaplan, *The Hermansky-Pudlak syndrome. Report of three cases and review of pathophysiology and management considerations.* Medicine (Baltimore), 1985. **64**(3): p. 192-202.

22. Oh, J., et al., *Positional cloning of a gene for Hermansky-Pudlak syndrome, a disorder of cytoplasmic organelles.* Nat Genet, 1996. **14**(3): p. 300-6.

23. Schneider, E.L., et al., *Severe pulmonary involvement in adult Gaucher's disease. Report of three cases and review of the literature.* Am J Med, 1977. **63**(3): p. 475-80.

24. Nogee, L.M., et al., *A mutation in the surfactant protein C gene associated with familial interstitial lung disease.* N Engl J Med, 2001. **344**(8): p. 573-9.

25. Thomas, A.Q., et al., *Heterozygosity for a surfactant protein C gene mutation associated with usual interstitial pneumonitis and cellular nonspecific interstitial pneumonitis in one kindred.* Am J Respir Crit Care Med, 2002. **165**(9): p. 1322-8.

26. Kipling, D., *Telomerase: immortality enzyme or oncogene?* Nat Genet, 1995. **9**(2): p. 104-6.

27. Tsakiri, K.D., et al., *Adult-onset pulmonary fibrosis caused by mutations in telomerase.* Proc Natl Acad Sci U S A, 2007. **104**(18): p. 7552-7.

28. Armanios, M.Y., et al., *Telomerase mutations in families with idiopathic pulmonary fibrosis.* N Engl J Med, 2007. **356**(13): p. 1317-26.

29. Keogh, B.A. and R.G. Crystal, *Alveolitis: the key to the interstitial lung disorders.* Thorax, 1982. **37**(1): p. 1-10.

30. Crystal, R.G., et al., *Idiopathic pulmonary fibrosis. Clinical, histologic, radiographic, physiologic, scintigraphic, cytologic, and biochemical aspects.* Ann Intern Med, 1976. **85**(6): p. 769-88.

31. Chilosi, M., et al., *Abnormal re-epithelialization and lung remodeling in idiopathic pulmonary fibrosis: the role of deltaN-p63.* Lab Invest, 2002. **82**(10): p. 1335-45.

32. White, E.S., M.H. Lazar, and V.J. Thannickal, *Pathogenetic mechanisms in usual interstitial pneumonia/idiopathic pulmonary fibrosis.* J Pathol, 2003. **201**(3): p. 343-54.

33. Egan, J.J., A.A. Woodcock, and J.P. Stewart, *Viruses and idiopathic pulmonary fibrosis.* Eur Respir J, 1997. **10**(7): p. 1433-7.

34. Cantin, A.M., et al., *Oxidant-mediated epithelial cell injury in idiopathic pulmonary fibrosis.* J Clin Invest, 1987. **79**(6): p. 1665-73.

35. Cantin, A.M., R.C. Hubbard, and R.G. Crystal, *Glutathione deficiency in the epithelial lining fluid of the lower respiratory tract in idiopathic pulmonary fibrosis.* Am Rev Respir Dis, 1989. **139**(2): p. 370-2.

36. Giaid, A., et al., *Expression of endothelin-1 in lungs of patients with cryptogenic fibrosing alveolitis.* Lancet, 1993. **341**(8860): p. 1550-4.

37. Kapanci, Y., et al., *Cytoskeletal protein modulation in pulmonary alveolar myofibroblasts during idiopathic pulmonary fibrosis. Possible role of transforming growth factor beta and tumor necrosis factor alpha.* Am J Respir Crit Care Med, 1995. **152**(6 Pt 1): p. 2163-9.

38. Xu, Y.D., et al., *Release of biologically active TGF-beta1 by alveolar epithelial cells results in pulmonary fibrosis.* Am J Physiol Lung Cell Mol Physiol, 2003. **285**(3): p. L527-39.

39. Kwong, K.Y., et al., *Expression of transforming growth factor beta (TGF-beta1) in human epithelial alveolar cells: a pro-inflammatory mediator independent pathway.* Life Sci, 2004. **74**(24): p. 2941-57.

40. Waghray, M., et al., *Hydrogen peroxide is a diffusible paracrine signal for the induction of epithelial cell death by activated myofibroblasts.* Faseb J, 2005. **19**(7): p. 854-6.

41. Khalil, N., et al., *Differential expression of transforming growth factor-beta type I and II receptors by pulmonary cells in bleomycin-induced lung injury: correlation with repair and fibrosis.* Exp Lung Res, 2002. **28**(3): p. 233-50.

42. du Bois, R.M. and A.U. Wells, *Cryptogenic fibrosing alveolitis/idiopathic pulmonary fibrosis.* Eur Respir J Suppl, 2001. **32**: p. 43s-55s.

43. Kasper, M. and G. Haroske, *Alterations in the alveolar epithelium after injury leading to pulmonary fibrosis.* Histol Histopathol, 1996. **11**(2): p. 463-83.

44. Strieter, R.M. and B. Mehrad, *New mechanisms of pulmonary fibrosis.* Chest, 2009. **136**(5): p. 1364-70.

45. Pardo, A. and M. Selman, *Matrix metalloproteases in aberrant fibrotic tissue remodeling.* Proc Am Thorac Soc, 2006. **3**(4): p. 383-8.

46. Barbas-Filho, J.V., et al., *Evidence of type II pneumocyte apoptosis in the pathogenesis of idiopathic pulmonary fibrosis (IFP)/usual interstitial pneumonia (UIP).* J Clin Pathol, 2001. **54**(2): p. 132-8.

47. Uhal, B.D., et al., *Alveolar epithelial cell death adjacent to underlying myofibroblasts in advanced fibrotic human lung.* Am J Physiol, 1998. **275**(6 Pt 1): p. L1192-9.

48. Plataki, M., et al., *Expression of apoptotic and antiapoptotic markers in epithelial cells in idiopathic pulmonary fibrosis.* Chest, 2005. **127**(1): p. 266-74.

49. Hagimoto, N., et al., *Induction of apoptosis and pulmonary fibrosis in mice in response to ligation of Fas antigen.* Am J Respir Cell Mol Biol, 1997. **17**(3): p. 272-8.

50. Yoshida, K., et al., *MAP kinase activation and apoptosis in lung tissues from patients with idiopathic pulmonary fibrosis.* J Pathol, 2002. **198**(3): p. 388-96.

51. Tanaka, T., et al., *Resistance to Fas-mediated apoptosis in human lung fibroblast.* Eur Respir J, 2002. **20**(2): p. 359-68.

52. McAnulty, R.J., *Fibroblasts and myofibroblasts: their source, function and role in disease.* Int J Biochem Cell Biol, 2007. **39**(4): p. 666-71.

53. Xu, S.W., et al., *Endothelin-1 induces expression of matrix-associated genes in lung fibroblasts through MEK/ERK.* J Biol Chem, 2004. **279**(22): p. 23098-103.

54. Jain, R., et al., *Endothelin-1 induces alveolar epithelial-mesenchymal transition through endothelin type A receptor-mediated production of TGF-beta1.* Am J Respir Cell Mol Biol, 2007. **37**(1): p. 38-47.

55. Saleh, D., et al., *Elevated expression of endothelin-1 and endothelin-converting enzyme-1 in idiopathic pulmonary fibrosis: possible involvement of proinflammatory cytokines.* Am J Respir Cell Mol Biol, 1997. **16**(2): p. 187-93.

56. Shahar, I., et al., *Effect of endothelin-1 on alpha-smooth muscle actin expression and on alveolar fibroblasts proliferation in interstitial lung diseases.* Int J Immunopharmacol, 1999. **21**(11): p. 759-75.

57. Uguccioni, M., et al., *Endothelin-1 in idiopathic pulmonary fibrosis.* J Clin Pathol, 1995. **48**(4): p. 330-4.

58. Reichenberger, F., et al., *Different expression of endothelin in the bronchoalveolar lavage in patients with pulmonary diseases.* Lung, 2001. **179**(3): p. 163-74.

59. Park, S.H., et al., *Increased endothelin-1 in bleomycin-induced pulmonary fibrosis and the effect of an endothelin receptor antagonist.* Am J Respir Crit Care Med, 1997. **156**(2 Pt 1): p. 600-8.

60. Mutsaers, S.E., et al., *Increased endothelin-1 and its localization during the development of bleomycin-induced pulmonary fibrosis in rats.* Am J Respir Cell Mol Biol, 1998. **18**(5): p. 611-9.

61. Wendel, M., et al., *Localization of endothelin receptors in bleomycin-induced pulmonary fibrosis in the rat.* Histochem Cell Biol, 2004. **122**(5): p. 507-17.

62. Hocher, B., et al., *Pulmonary fibrosis and chronic lung inflammation in ET-1 transgenic mice.* Am J Respir Cell Mol Biol, 2000. **23**(1): p. 19-26.

63. Kaminski, N., et al., *Use of oligonucleotide microarrays to analyze gene expression patterns in pulmonary fibrosis reveals distinct patterns of gene expression in mice and humans.* Chest, 2002. **121**(3 Suppl): p. 31S-32S.

64. Wang, X.M., et al., *Caveolin-1: a critical regulator of lung fibrosis in idiopathic pulmonary fibrosis.* J Exp Med, 2006. **203**(13): p. 2895-906.

65. Englert, J.M., et al., *A role for the receptor for advanced glycation end products in idiopathic pulmonary fibrosis.* Am J Pathol, 2008. **172**(3): p. 583-91.

66. Selman, M., A. Pardo, and N. Kaminski, *Idiopathic pulmonary fibrosis: aberrant recapitulation of developmental programs?* PLoS Med, 2008. **5**(3): p. e62.

67. King, T.E., Jr., et al., *Idiopathic pulmonary fibrosis: relationship between histopathologic features and mortality.* Am J Respir Crit Care Med, 2001. **164**(6): p. 1025-32.

68. Cool, C.D., et al., *Fibroblast foci are not discrete sites of lung injury or repair: the fibroblast reticulum.* Am J Respir Crit Care Med, 2006. **174**(6): p. 654-8.

69. Schurch, W., T.A. Seemayer, and G. Gabbiani, *The myofibroblast: a quarter century after its discovery.* Am J Surg Pathol, 1998. **22**(2): p. 141-7.

70. Phan, S.H., *The myofibroblast in pulmonary fibrosis.* Chest, 2002. **122**(6 Suppl): p. 286S-289S.

71. Uhal, B.D., et al., *Fibroblasts isolated after fibrotic lung injury induce apoptosis of alveolar epithelial cells in vitro.* Am J Physiol, 1995. **269**(6 Pt 1): p. L819-28.

72. Selman, M., et al., *TIMP-1, -2, -3, and -4 in idiopathic pulmonary fibrosis. A prevailing nondegradative lung microenvironment?* Am J Physiol Lung Cell Mol Physiol, 2000. **279**(3): p. L562-74.

73. Hu, B., Z. Wu, and S.H. Phan, *Smad3 mediates transforming growth factor-beta-induced alpha-smooth muscle actin expression.* Am J Respir Cell Mol Biol, 2003. **29**(3 Pt 1): p. 397-404.

74. Strieter, R.M., *What differentiates normal lung repair and fibrosis? Inflammation, resolution of repair, and fibrosis.* Proc Am Thorac Soc, 2008. **5**(3): p. 305-10.

75. Bucala, R., et al., *Circulating fibrocytes define a new leukocyte subpopulation that mediates tissue repair.* Mol Med, 1994. **1**(1): p. 71-81.

76. Epperly, M.W., et al., *Bone marrow origin of myofibroblasts in irradiation pulmonary fibrosis.* Am J Respir Cell Mol Biol, 2003. **29**(2): p. 213-24.

77. Direkze, N.C., et al., *Multiple organ engraftment by bone-marrow-derived myofibroblasts and fibroblasts in bone-marrow-transplanted mice.* Stem Cells, 2003. **21**(5): p. 514-20.

78. Mehrad, B., et al., *Circulating peripheral blood fibrocytes in human fibrotic interstitial lung disease.* Biochem Biophys Res Commun, 2007. **353**(1): p. 104-8.

79. Andersson-Sjoland, A., et al., *Fibrocytes are a potential source of lung fibroblasts in idiopathic pulmonary fibrosis.* Int J Biochem Cell Biol, 2008. **40**(10): p. 2129-40.

80. Moeller, A., et al., *Circulating fibrocytes are an indicator of poor prognosis in idiopathic pulmonary fibrosis.* Am J Respir Crit Care Med, 2009. **179**(7): p. 588-94.

81. Adamson, I.Y., L. Young, and D.H. Bowden, *Relationship of alveolar epithelial injury and repair to the induction of pulmonary fibrosis.* Am J Pathol, 1988. **130**(2): p. 377-83.

82. Kim, K.K., et al., *Alveolar epithelial cell mesenchymal transition develops in vivo during pulmonary fibrosis and is regulated by the extracellular matrix.* Proc Natl Acad Sci U S A, 2006. **103**(35): p. 13180-5.

83. Kim, K.K., et al., *Epithelial cell alpha3beta1 integrin links beta-catenin and Smad signaling to promote myofibroblast formation and pulmonary fibrosis.* J Clin Invest, 2009. **119**(1): p. 213-24.

84. Tanjore, H., et al., *Contribution of epithelial-derived fibroblasts to bleomycin-induced lung fibrosis.* Am J Respir Crit Care Med, 2009. **180**(7): p. 657-65.

85. Sheppard, D., *Transforming growth factor beta: a central modulator of pulmonary and airway inflammation and fibrosis.* Proc Am Thorac Soc, 2006. **3**(5): p. 413-7.

86. Broekelmann, T.J., et al., *Transforming growth factor beta 1 is present at sites of extracellular matrix gene expression in human pulmonary fibrosis.* Proc Natl Acad Sci U S A, 1991. **88**(15): p. 6642-6.

87. Kapanci, Y., et al., *Phenotypic modulation of alveolar myofibroblasts in transplanted human lungs.* Mod Pathol, 1997. **10**(11): p. 1134-42.

88. Khalil, N., et al., *TGF-beta 1, but not TGF-beta 2 or TGF-beta 3, is differentially present in epithelial cells of advanced pulmonary fibrosis: an immunohistochemical study.* Am J Respir Cell Mol Biol, 1996. **14**(2): p. 131-8.

89. Khalil, N., et al., *Biological effects of transforming growth factor-beta(1) in idiopathic pulmonary fibrosis may be regulated by the activation of latent transforming growth factor-beta(1) and the differential expression of transforming growth factor-beta receptors.* Chest, 2001. **120**(1 Suppl): p. 48S.

90. Khalil, N., et al., *Regulation of alveolar macrophage transforming growth factor-beta secretion by corticosteroids in bleomycin-induced pulmonary inflammation in the rat.* J Clin Invest, 1993. **92**(4): p. 1812-8.

91. Sime, P.J., et al., *Adenovector-mediated gene transfer of active transforming growth factor-beta1 induces prolonged severe fibrosis in rat lung.* J Clin Invest, 1997. **100**(4): p. 768-76.

92. Gauldie, J., et al., *Smad3 signaling involved in pulmonary fibrosis and emphysema.* Proc Am Thorac Soc, 2006. **3**(8): p. 696-702.

93. Venkatesan, N., L. Pini, and M.S. Ludwig, *Changes in Smad expression and subcellular localization in bleomycin-induced pulmonary fibrosis.* Am J Physiol Lung Cell Mol Physiol, 2004. **287**(6): p. L1342-7.

94. Gu, L., et al., *Effect of TGF-beta/Smad signaling pathway on lung myofibroblast differentiation.* Acta Pharmacol Sin, 2007. **28**(3): p. 382-91.

95. Zhao, J., et al., *Smad3 deficiency attenuates bleomycin-induced pulmonary fibrosis in mice.* Am J Physiol Lung Cell Mol Physiol, 2002. **282**(3): p. L585-93.

96. Zhao, Y. and D.A. Geverd, *Regulation of Sm ad3 e xpression i n bl eomycin-induced pulmonary fibrosis: a ne gative feedback loop of TGF-beta s ignaling.* Biochem Biophys Res Commun, 2002. **294**(2): p. 319-23.

97. Nakao, A., et al., *Transient gene transfer and expression of Smad7 prevents bleomycin-induced lung fibrosis in mice.* J Clin Invest, 1999. **104**(1): p. 5-11.

98. Xu, G.P., et al., *The Effect of TGF-beta1 and S MAD7 ge ne t ransfer on the phe notypic changes of rat alveolar epithelial cells.* Cell Mol Biol Lett, 2007.

99. Moon, R.T., et al., *WNT and be ta-catenin s ignalling: di seases and t herapies.* Nat Rev Genet, 2004. **5**(9): p. 691-701.

100. Logan, C.Y. and R. Nusse, *The Wnt signaling pathway in development and disease.* Annu Rev Cell Dev Biol, 2004. **20**: p. 781-810.

101. Chilosi, M., et al., *Aberrant W nt/beta-catenin pat hway ac tivation in i diopathic pulmonary fibrosis.* Am J Pathol, 2003. **162**(5): p. 1495-502.

102. Crawford, H.C., et al., *The m etalloproteinase m atrilysin is a target of be ta-catenin transactivation in intestinal tumors.* Oncogene, 1999. **18**(18): p. 2883-91.

103. Lewis, C.C., et al., *Disease-specific gene expression profiling in multiple models of lung disease.* Am J Respir Crit Care Med, 2008. **177**(4): p. 376-87.

104. Konigshoff, M., et al., *WNT1-inducible signaling protein-1 mediates pulmonary fibrosis in mice and i s upregulated in humans with idiopathic pulmonary fibrosis.* J Clin Invest, 2009. **119**(4): p. 772-87.

105. Kalluri, R. and E.G. Neilson, *Epithelial-mesenchymal transition and i ts implications for fibrosis.* J Clin Invest, 2003. **112**(12): p. 1776-84.

106. Acloque, H., et al., *Epithelial-mesenchymal transitions: the importance of changing cell state in development and disease.* J Clin Invest, 2009. **119**(6): p. 1438-49.

107. Zeisberg, M. and E.G. Neilson, *Biomarkers for epithelial-mesenchymal transitions.* J Clin Invest, 2009. **119**(6): p. 1429-37.

108. Kalluri, R. and R.A. Weinberg, *The bas ics of e pithelial-mesenchymal t ransition.* J Clin Invest, 2009. **119**(6): p. 1420-8.

109. Kalluri, R., *EMT: w hen epithelial cells de cide to become mesenchymal-like cells.* J Clin Invest, 2009. **119**(6): p. 1417-9.

110. Strutz, F., et al., *Role of bas ic f ibroblast gr owth f actor-2 i n e pithelial-mesenchymal transformation.* Kidney Int, 2002. **61**(5): p. 1714-28.

111. Venkov, C.D., et al., *A proximal activator of transcription in epithelial-mesenchymal transition.* J Clin Invest, 2007. **117**(2): p. 482-91.

112. Thuault, S., et al., *Transforming growth factor-beta employs HMGA2 to elicit epithelial-mesenchymal transition.* J Cell Biol, 2006. **174**(2): p. 175-83.

113. Reeves, R., *Molecular biology of HMGA proteins: hubs of nuclear function.* Gene, 2001. **277**(1-2): p. 63-81.

114. Reeves, R., D.D. Edberg, and Y. Li, *Architectural transcription factor HMGI(Y) promotes tumor progression and mesenchymal transition of human epithelial cells.* Mol Cell Biol, 2001. **21**(2): p. 575-94.

115. Sgarra, R., et al., *Nuclear phosphoproteins HMGA and their relationship with chromatin structure and cancer.* FEBS Lett, 2004. **574**(1-3): p. 1-8.

116. Peinado, H., D. Olmeda, and A. Cano, *Snail, Zeb and bHLH factors in tumour progression: an alliance against the epithelial phenotype?* Nat Rev Cancer, 2007. **7**(6): p. 415-28.

117. Thuault, S., et al., *HMGA2 and Smads co-regulate SNAIL1 expression during induction of epithelial-to-mesenchymal transition.* J Biol Chem, 2008. **283**(48): p. 33437-46.

118. Kondo, M., et al., *A role for Id in the regulation of TGF-beta-induced epithelial-mesenchymal transdifferentiation.* Cell Death Differ, 2004. **11**(10): p. 1092-101.

119. Kowanetz, M., et al., *Id2 and Id3 define the potency of cell proliferation and differentiation responses to transforming growth factor beta and bone morphogenetic protein.* Mol Cell Biol, 2004. **24**(10): p. 4241-54.

120. Burk, U., et al., *A reciprocal repression between ZEB1 and members of the miR-200 family promotes EMT and invasion in cancer cells.* EMBO Rep, 2008. **9**(6): p. 582-9.

121. Korpal, M., et al., *The miR-200 family inhibits epithelial-mesenchymal transition and cancer cell migration by direct targeting of E-cadherin transcriptional repressors ZEB1 and ZEB2.* J Biol Chem, 2008. **283**(22): p. 14910-4.

122. Park, S.M., et al., *The miR-200 family determines the epithelial phenotype of cancer cells by targeting the E-cadherin repressors ZEB1 and ZEB2.* Genes Dev, 2008. **22**(7): p. 894-907.

123. Gregory, P.A., et al., *The miR-200 family and miR-205 regulate epithelial to mesenchymal transition by targeting ZEB1 and SIP1.* Nat Cell Biol, 2008. **10**(5): p. 593-601.

124. Iorio, M.V., et al., *MicroRNA gene expression deregulation in human breast cancer.* Cancer Res, 2005. **65**(16): p. 7065-70.

125. Si, M.L., et al., *miR-21-mediated tumor growth.* Oncogene, 2007. **26**(19): p. 2799-803.

126. Kong, W., et al., *MicroRNA-155 is regulated by the transforming growth factor beta/Smad pathway and contributes to epithelial cell plasticity by targeting RhoA.* Mol Cell Biol, 2008. **28**(22): p. 6773-84.

127. Hayashita, Y., et al., *A polycistronic microRNA cluster, miR-17-92, is overexpressed in human lung cancers and enhances cell proliferation.* Cancer Res, 2005. **65**(21): p. 9628-32.

128. Zavadil, J., et al., *Transforming growth factor-beta and microRNA:mRNA regulatory networks in epithelial plasticity.* Cells Tissues Organs, 2007. **185**(1-3): p. 157-61.

129. Asangani, I.A., et al., *MicroRNA-21 (miR-21) post-transcriptionally downregulates tumor suppressor Pdcd4 and stimulates invasion, intravasation and metastasis in colorectal cancer.* Oncogene, 2008. **27**(15): p. 2128-36.

130. Zhu, S., et al., *MicroRNA-21 targets the tumor suppressor gene tropomyosin 1 (TPM1).* J Biol Chem, 2007. **282**(19): p. 14328-36.

131. Pottier, N., et al., *Identification of keratinocyte growth factor as a target of microRNA-155 in lung fibroblasts: implication in epithelial-mesenchymal interactions.* PLoS One, 2009. **4**(8): p. e6718.

132. Kim, V.N., J. Han, and M.C. Siomi, *Biogenesis of small RNAs in animals.* Nat Rev Mol Cell Biol, 2009. **10**(2): p. 126-39.

133. Lagos-Quintana, M., et al., *Identification of novel genes coding for small expressed RNAs.* Science, 2001. **294**(5543): p. 853-8.

134. Lau, N.C., et al., *An abundant class of tiny RNAs with probable regulatory roles in Caenorhabditis elegans.* Science, 2001. **294**(5543): p. 858-62.

135. Lee, R.C. and V. Ambros, *An extensive class of small RNAs in Caenorhabditis elegans.* Science, 2001. **294**(5543): p. 862-4.

136. Reinhart, B.J., et al., *The 21-nucleotide let-7 RNA regulates developmental timing in Caenorhabditis elegans.* Nature, 2000. **403**(6772): p. 901-6.

137. Reinhart, B.J., et al., *MicroRNAs in plants.* Genes Dev, 2002. **16**(13): p. 1616-26.

138. Mourelatos, Z., et al., *miRNPs: a novel class of ribonucleoproteins containing numerous microRNAs.* Genes Dev, 2002. **16**(6): p. 720-8.

139. Lee, Y., et al., *MicroRNA genes are transcribed by RNA polymerase II.* Embo J, 2004. **23**(20): p. 4051-60.

140. Borchert, G.M., W. Lanier, and B.L. Davidson, *RNA polymerase III transcribes human microRNAs.* Nat Struct Mol Biol, 2006. **13**(12): p. 1097-101.

141. O'Donnell, K.A., et al., *c-Myc-regulated microRNAs modulate E2F1 expression.* Nature, 2005. **435**(7043): p. 839-43.

142. Gressner, O.A., R. Weiskirchen, and A.M. Gressner, *Evolving concepts of liver fibrogenesis provide new diagnostic and therapeutic options.* Comp Hepatol, 2007. **6**: p. 7.

143. Brueckner, B., et al., *The human let-7a-3 locus contains an epigenetically regulated microRNA gene with oncogenic function.* Cancer Res, 2007. **67**(4): p. 1419-23.

144. Winter, J., et al., *Many roads to maturity: microRNA biogenesis pathways and their regulation.* Nat Cell Biol, 2009. **11**(3): p. 228-34.

145. Kim, V.N., *MicroRNA biogenesis: coordinated cropping and dicing.* Nat Rev Mol Cell Biol, 2005. **6**(5): p. 376-85.

146. Roush, S. and F.J. Slack, *The let-7 family of microRNAs.* Trends Cell Biol, 2008. **18**(10): p. 505-16.

147. Pasquinelli, A.E., et al., *Conservation of the sequence and temporal expression of let-7 heterochronic regulatory RNA.* Nature, 2000. **408**(6808): p. 86-9.

148. Sokol, N.S., et al., *Drosophila let-7 microRNA is required for remodeling of the neuromusculature during metamorphosis.* Genes Dev, 2008. **22**(12): p. 1591-6.

149. Caygill, E.E. and L.A. Johnston, *Temporal regulation of metamorphic processes in Drosophila by the let-7 and miR-125 heterochronic microRNAs.* Curr Biol, 2008. **18**(13): p. 943-50.

150. Schulman, B.R., A. Esquela-Kerscher, and F.J. Slack, *Reciprocal expression of lin-41 and the microRNAs let-7 and mir-125 during mouse embryogenesis.* Dev Dyn, 2005. **234**(4): p. 1046-54.

151. Yu, F., et al., *let-7 regulates self renewal and tumorigenicity of breast cancer cells.* Cell, 2007. **131**(6): p. 1109-23.

152. Wulczyn, F.G., et al., *Post-transcriptional regulation of the let-7 microRNA during neural cell specification.* Faseb J, 2007. **21**(2): p. 415-26.

153. Yu, J., et al., *Induced pluripotent stem cell lines derived from human somatic cells.* Science, 2007. **318**(5858): p. 1917-20.

154. Hatfield, S. and H. Ruohola-Baker, *microRNA and stem cell function.* Cell Tissue Res, 2008. **331**(1): p. 57-66.

155. Esquela-Kerscher, A. and F.J. Slack, *Oncomirs - microRNAs with a role in cancer.* Nat Rev Cancer, 2006. **6**(4): p. 259-69.

156. Kloosterman, W.P. and R.H. Plasterk, *The diverse functions of microRNAs in animal development and disease.* Dev Cell, 2006. **11**(4): p. 441-50.

157. Lancman, J.J., et al., *Analysis of the regulation of lin-41 during chick and mouse limb development.* Dev Dyn, 2005. **234**(4): p. 948-60.

158. Ibarra, I., et al., *A role for microRNAs in maintenance of mouse mammary epithelial progenitor cells.* Genes Dev, 2007. **21**(24): p. 3238-43.

159. Reid, J.G., et al., *Mouse let-7 miRNA populations exhibit RNA editing that is constrained in the 5'-seed/cleavage/anchor regions and stabilize predicted mmu-let-7a:mRNA duplexes.* Genome Res, 2008. **18**(10): p. 1571-81.

160. Rodriguez, A., et al., *Identification of mammalian microRNA host genes and transcription units.* Genome Res, 2004. **14**(10A): p. 1902-10.

161. Newman, M.A., J.M. Thomson, and S.M. Hammond, *Lin-28 interaction with the Let-7 precursor loop mediates regulated microRNA processing.* Rna, 2008. **14**(8): p. 1539-49.

162. Viswanathan, S.R., G.Q. Daley, and R.I. Gregory, *Selective blockade of microRNA processing by Lin28.* Science, 2008. **320**(5872): p. 97-100.

163. Rybak, A., et al., *A feedback loop comprising lin-28 and let-7 controls pre-let-7 maturation during neural stem-cell commitment.* Nat Cell Biol, 2008. **10**(8): p. 987-93.

164. Heo, I., et al., *Lin28 mediates the terminal uridylation of let-7 precursor MicroRNA.* Mol Cell, 2008. **32**(2): p. 276-84.

165. Katzenstein, A.L. and J.L. Myers, *Idiopathic pulmonary fibrosis: clinical relevance of pathologic classification.* Am J Respir Crit Care Med, 1998. **157**(4 Pt 1): p. 1301-15.

166. Segal, E., et al., *A module map showing conditional activity of expression modules in cancer.* Nat Genet, 2004. **36**(10): p. 1090-8.

167. Kent, W.J., et al., *The human genome browser at UCSC.* Genome Res, 2002. **12**(6): p. 996-1006.

168. Baskerville, S. and D.P. Bartel, *Microarray profiling of microRNAs reveals frequent coexpression with neighboring miRNAs and host genes.* Rna, 2005. **11**(3): p. 241-7.

169. Corcoran, D.L., et al., *Footer: a quantitative comparative genomics method for efficient recognition of cis-regulatory elements.* Genome Res, 2005. **15**(6): p. 840-7.

170. Lee, T.I., et al., *Transcriptional regulatory networks in Saccharomyces cerevisiae.* Science, 2002. **298**(5594): p. 799-804.

171. Andrews, N.C. and D.V. Faller, *A rapid micropreparation technique for extraction of DNA-binding proteins from limiting numbers of mammalian cells.* Nucleic Acids Res, 1991. **19**(9): p. 2499.

172. Tzouvelekis, A., et al., *Comparative expression profiling in pulmonary fibrosis suggests a role of hypoxia-inducible factor-1alpha in disease pathogenesis.* Am J Respir Crit Care Med, 2007. **176**(11): p. 1108-19.

173. Krutzfeldt, J., et al., *Silencing of microRNAs in vivo with 'antagomirs'.* Nature, 2005. **438**(7068): p. 685-9.

174. Gomori, G., *A rapid one-step trichrome stain.* Am J Clin Pathol, 1950. **20**(7): p. 661-4.

175. Zhou, X., et al., *Characterization and identification of microRNA core promoters in four model species.* PLoS Comput Biol, 2007. **3**(3): p. e37.

176. Mayr, C., M.T. Hemann, and D.P. Bartel, *Disrupting the pairing between let-7 and Hmga2 enhances oncogenic transformation.* Science, 2007. **315**(5818): p. 1576-9.

177. Johnson, S.M., et al., *RAS is regulated by the let-7 microRNA family.* Cell, 2005. **120**(5): p. 635-47.

178. Watanabe, S., et al., *HMGA2 maintains oncogenic RAS-induced epithelial-mesenchymal transition in human pancreatic cancer cells.* Am J Pathol, 2009. **174**(3): p. 854-68.

179. Mott, J.L., et al., *mir-29 regulates Mcl-1 protein expression and apoptosis.* Oncogene, 2007. **26**(42): p. 6133-40.

180. Chen, F., et al., *Repression of Smad2 and Smad3 transactivating activity by association with a novel splice variant of CCAAT-binding factor C subunit.* Biochem J, 2002. **364**(Pt 2): p. 571-7.

181. Nawshad, A., et al., *Transforming growth factor-beta signaling during epithelial-mesenchymal transformation: implications for embryogenesis and tumor metastasis.* Cells Tissues Organs, 2005. **179**(1-2): p. 11-23.

182. Corcoran, D.L., et al., *Features of mammalian microRNA promoters emerge from polymerase II chromatin immunoprecipitation data.* PLoS One, 2009. **4**(4): p. e5279.

183. Marson, A., et al., *Connecting microRNA genes to the core transcriptional regulatory circuitry of embryonic stem cells.* Cell, 2008. **134**(3): p. 521-33.

184. Calin, G.A., et al., *Human microRNA genes are frequently located at fragile sites and genomic regions involved in cancers.* Proc Natl Acad Sci U S A, 2004. **101**(9): p. 2999-3004.

185. Thomson, J.M., et al., *Extensive post-transcriptional regulation of microRNAs and its implications for cancer.* Genes Dev, 2006. **20**(16): p. 2202-7.

186. Johnson, C.D., et al., *The let-7 microRNA represses cell proliferation pathways in human cells.* Cancer Res, 2007. **67**(16): p. 7713-22.

187. Shell, S., et al., *Let-7 expression defines two differentiation stages of cancer.* Proc Natl Acad Sci U S A, 2007. **104**(27): p. 11400-5.

188. Zhou, X., et al., *Mutations responsible for the mouse pygmy phenotype in the developmentally regulated factor HMGI-C.* Nature, 1995. **376**(6543): p. 771-4.

189. Duisters, R.F., et al., *miR-133 and miR-30 regulate connective tissue growth factor: implications for a role of microRNAs in myocardial matrix remodeling.* Circ Res, 2009. **104**(2): p. 170-8, 6p following 178.

190. Grotendorst, G.R., H. Okochi, and N. Hayashi, *A novel transforming growth factor beta response element controls the expression of the connective tissue growth factor gene.* Cell Growth Differ, 1996. **7**(4): p. 469-80.

191. Pan, L.H., et al., *Type II alveolar epithelial cells and interstitial fibroblasts express connective tissue growth factor in IPF.* Eur Respir J, 2001. **17**(6): p. 1220-7.

192. Izzotti, A., et al., *Downregulation of microRNA expression in the lungs of rats exposed to cigarette smoke.* Faseb J, 2009. **23**(3): p. 806-12.

193. Schembri, F., et al., *MicroRNAs as modulators of smoking-induced gene expression changes in human airway epithelium.* Proc Natl Acad Sci U S A, 2009. **106**(7): p. 2319-24.

194. Childs, G., et al., *Low-level expression of microRNAs let-7d and miR-205 are prognostic markers of head and neck squamous cell carcinoma.* Am J Pathol, 2009. **174**(3): p. 736-45.

195. Esquela-Kerscher, A., et al., *The let-7 microRNA reduces tumor growth in mouse models of lung cancer.* Cell Cycle, 2008. **7**(6): p. 759-64.

196. Fabbri, M., et al., *MicroRNA-29 family reverts aberrant methylation in lung cancer by targeting DNA methyltransferases 3A and 3B.* Proc Natl Acad Sci U S A, 2007. **104**(40): p. 15805-10.

197. Ichimi, T., et al., *Identification of novel microRNA targets based on microRNA signatures in bladder cancer.* Int J Cancer, 2009. **125**(2): p. 345-52.

198. Ji, J., et al., *MicroRNA expression, survival, and response to interferon in liver cancer.* N Engl J Med, 2009. **361**(15): p. 1437-47.

199. Pekarsky, Y., et al., *Tcl1 expression in chronic lymphocytic leukemia is regulated by miR-29 and miR-181.* Cancer Res, 2006. **66**(24): p. 11590-3.

200. Takamizawa, J., et al., *Reduced expression of the let-7 microRNAs in human lung cancers in association with shortened postoperative survival.* Cancer Res, 2004. **64**(11): p. 3753-6.

201. Wu, F., et al., *MicroRNA-mediated regulation of Ubc9 expression in cancer cells.* Clin Cancer Res, 2009. **15**(5): p. 1550-7.